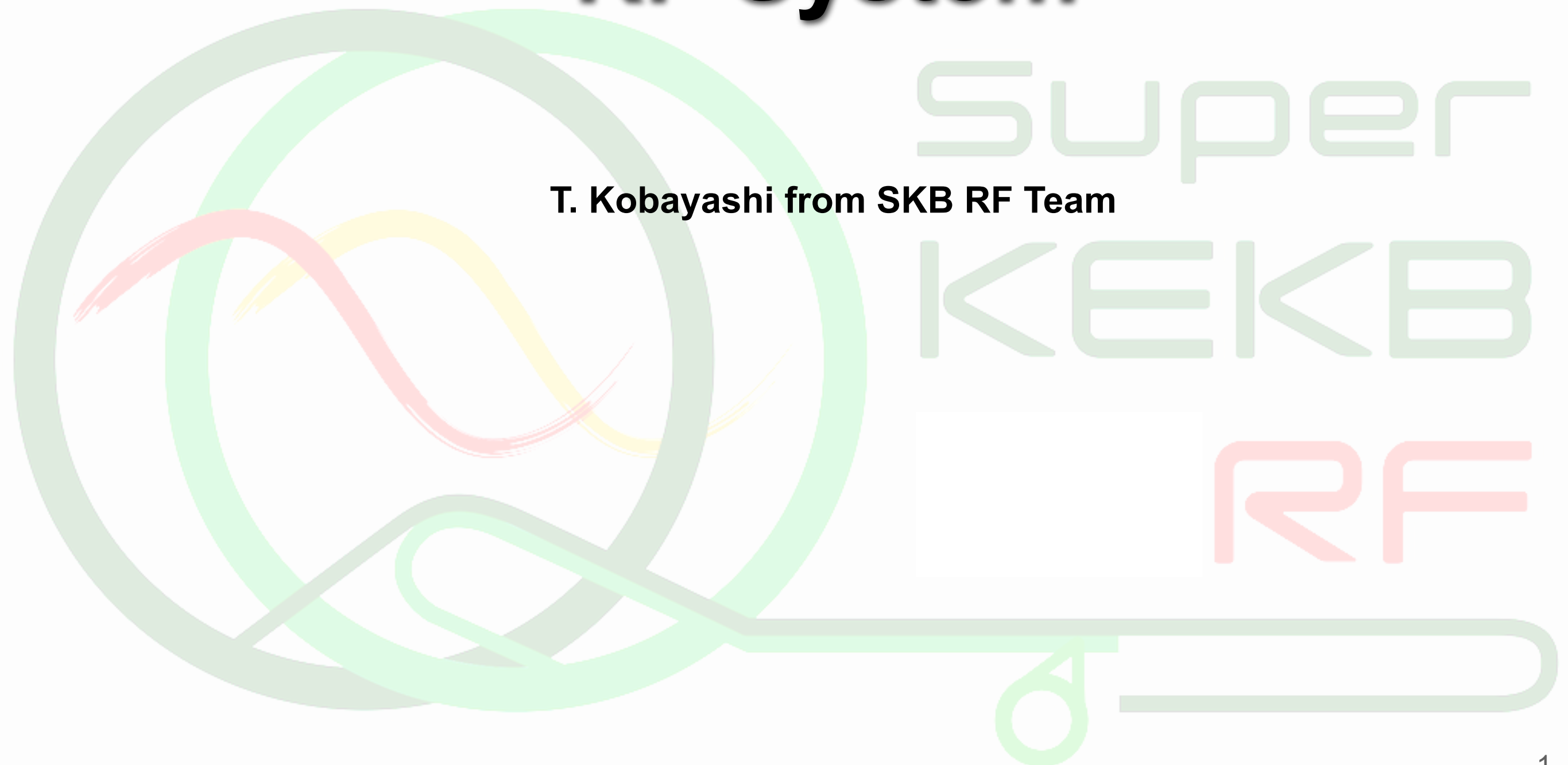


# Operation Status of RF System

T. Kobayashi from SKB RF Team



SUPER  
KEKB  
RF

# Outline

**1. Introduction**

**2. Beam Operation Status**

**3. Status of High Power RF System (Kly, KPS, WG)**

**4. Status of Low Level RF Control System**

**5. Bunch Gap Transient Effect on Beam Phase (as a future issue)**

**6. Summary**

Following talks:

- Superconducting Cavity (M. Nishiwaki)
- ARES -Normal Conducting- Cavity (T. Abe)

# Cavity Types

**ARES**  
@Oho, Fuji

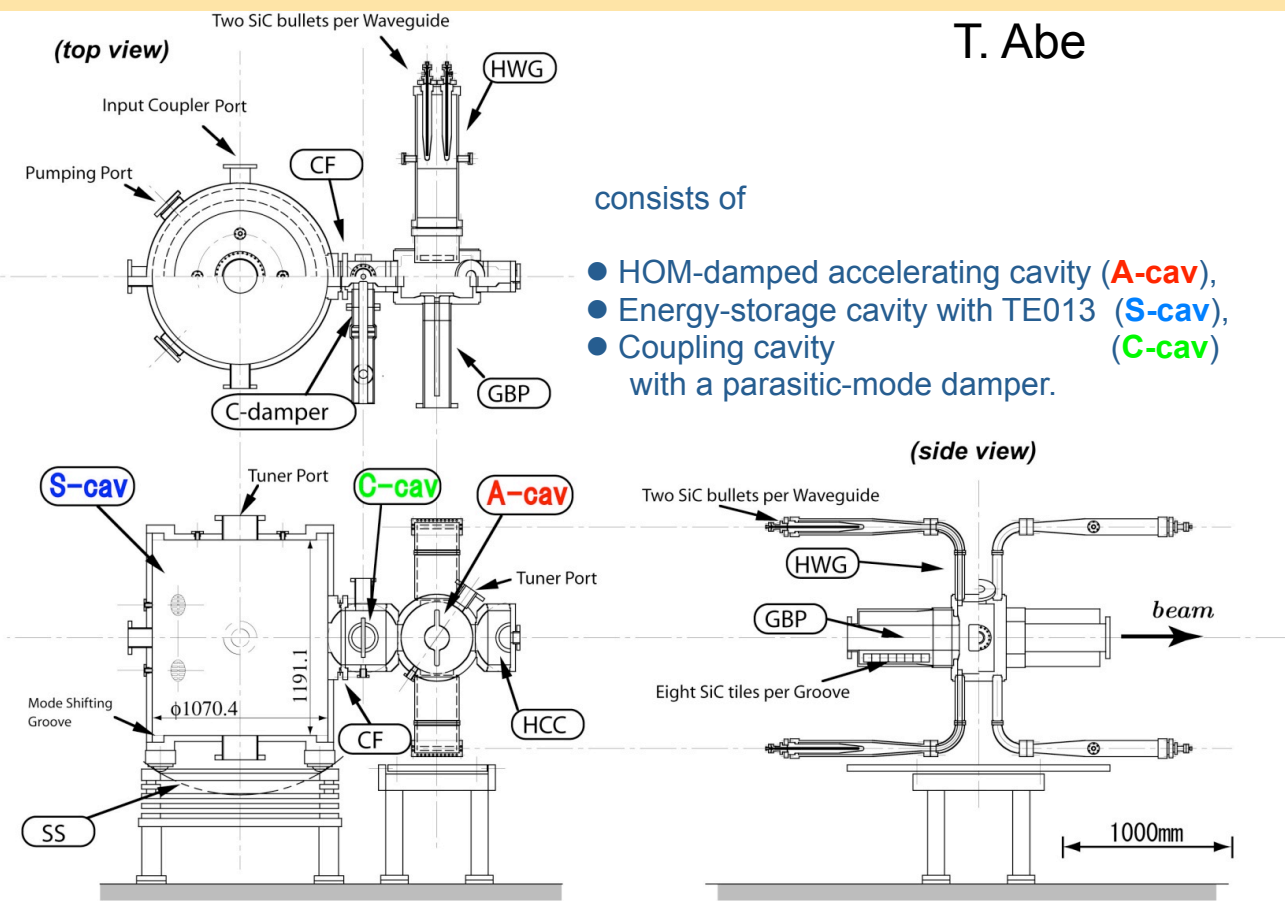
T. Abe

**SCC**  
@Nikko

M. Nishiwaki

Accelerator Resonantly-coupled with Energy Storage  
3-cavity system stabilized with the  $\pi/2$ -mode operation

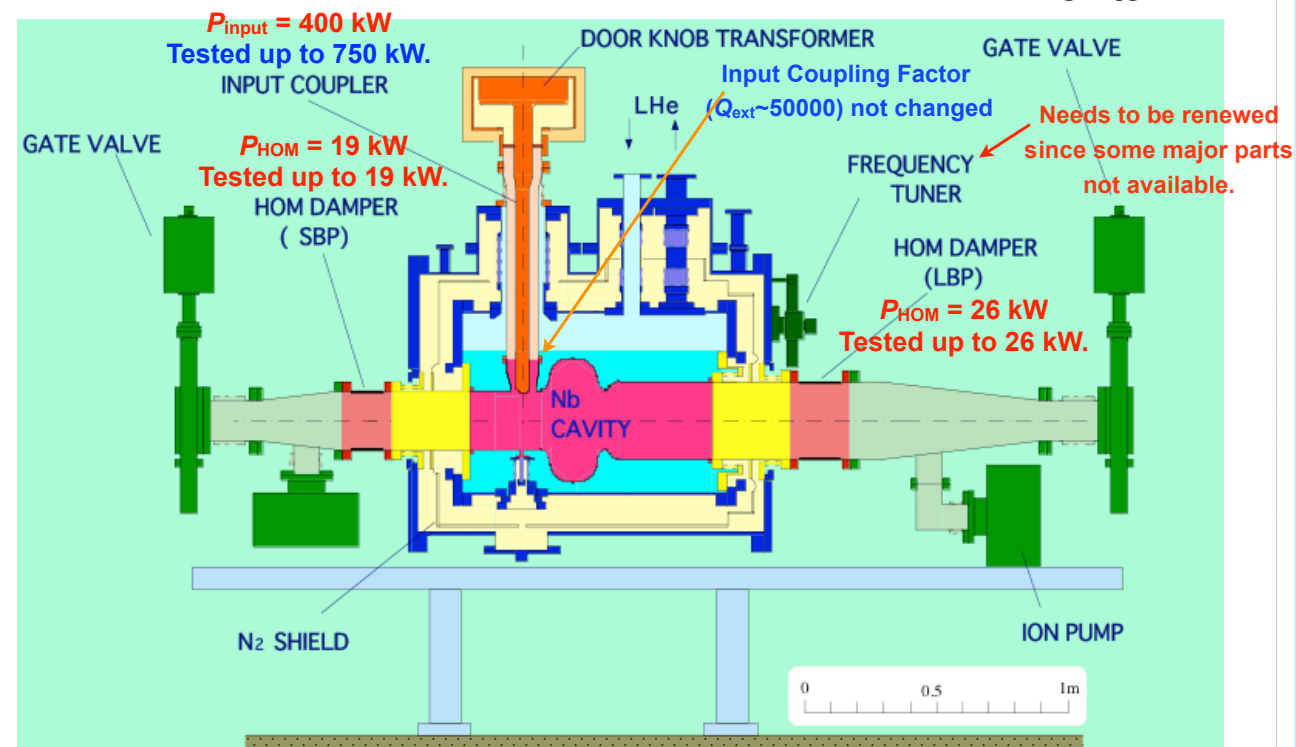
Successful Operation of the 32 ARES Cavities at KEKB



T. Abe

8 modules have been installed in Nikko for HER.

Y. Morita

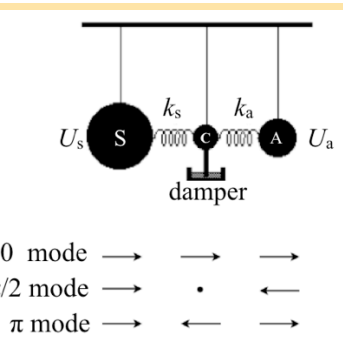


$V_c = 1.5 \text{ MV}$ ,  $P_{\text{beam}} = 400 \text{ kW /cavity}$



Cavity parameters of the KEKB Superconducting cavity

Frequency	508.8	MHz
Gap length	243	mm
Diameter of aperture	220	mm
$R/Q$	93	Ohms
Geometrical factor	251	Ohms
$E_{\text{sp}}/E_{\text{acc}}$	1.84	
$H_{\text{sp}}/E_{\text{acc}}$	40.3	Gauss/(MV/m)

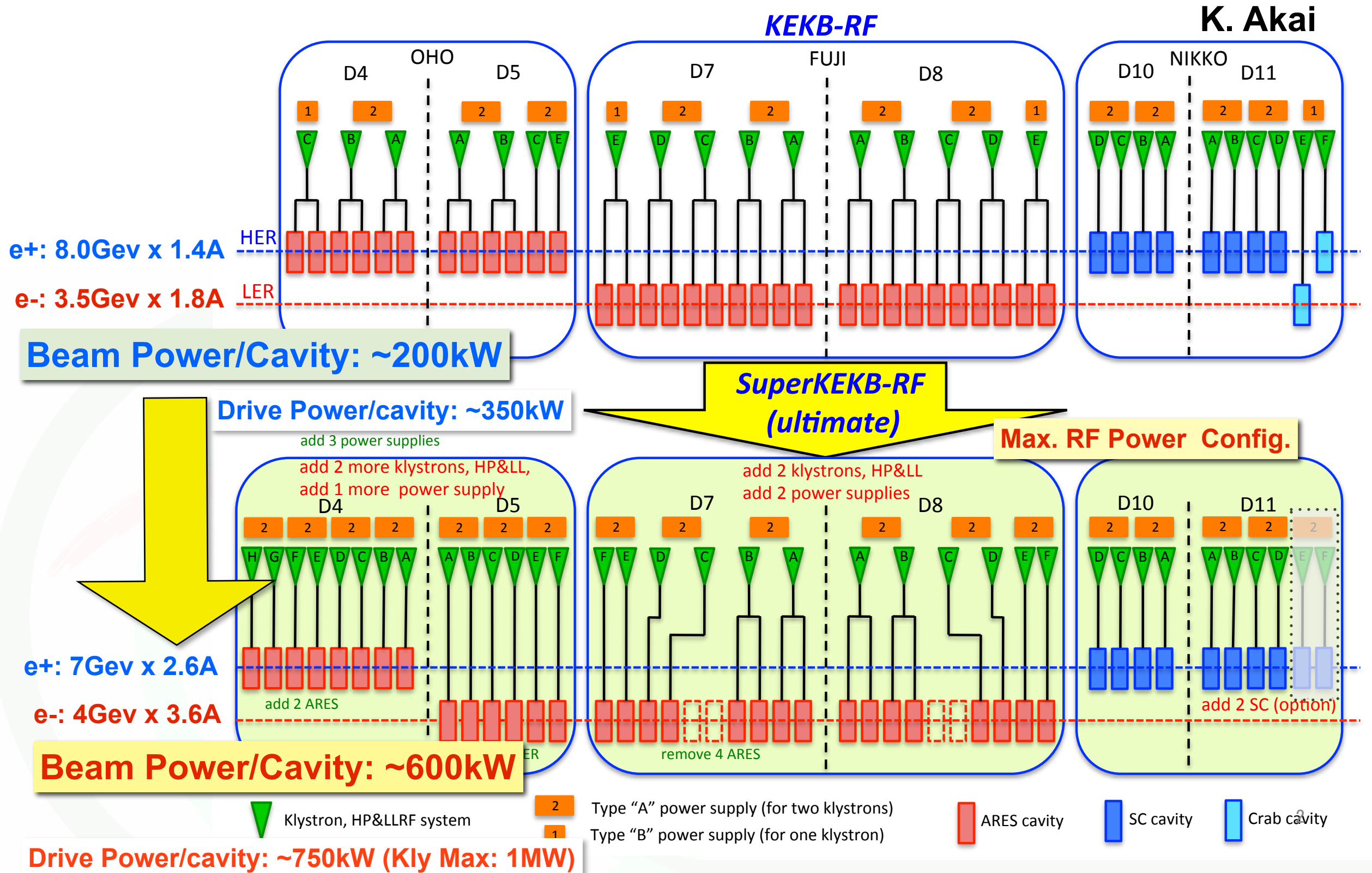


ARES parameters	
$f_{\text{RF}}$	508MHz
$U_s / U_a$	9
$R/Q_0$	15 $\Omega$ for the $\pi/2$ mode
$Q_0$	$1.1 \times 10^5$
$V_c$	0.5 MV
$P_c$	150 kW 60 kW (A) + 90 kW (S)



Basically, KEKB RF systems are reused with reinforcement for SuperKEKB.

# Intro.: RF System Arrangement (ultimate)



➔ **One-to-one configuration** for every ARES (One klystron drives one cavity unit).

➔ **Upgrade** of input coupler for the ARES (up to  $\beta \sim 6$ , 800-kW input power capable)

➔ **Addition** of new **HOM Damper** for the SCC as a measure against beam-induced HOM-power rising.

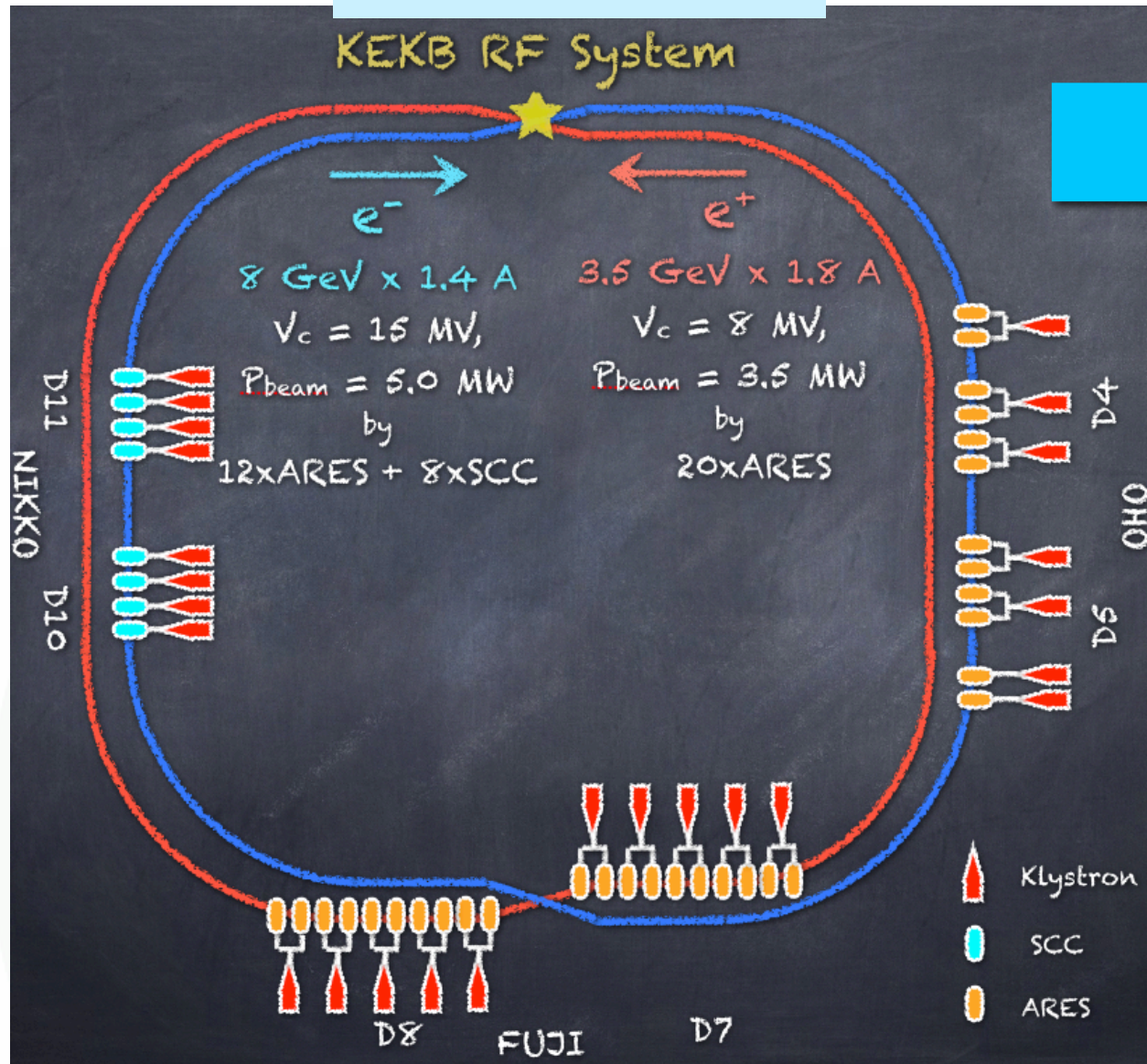
➔ **add 9 klystrons and 3 PS's more.**  
 • increase and reinforce WG systems.

# RF System Arrangement for Phase-I

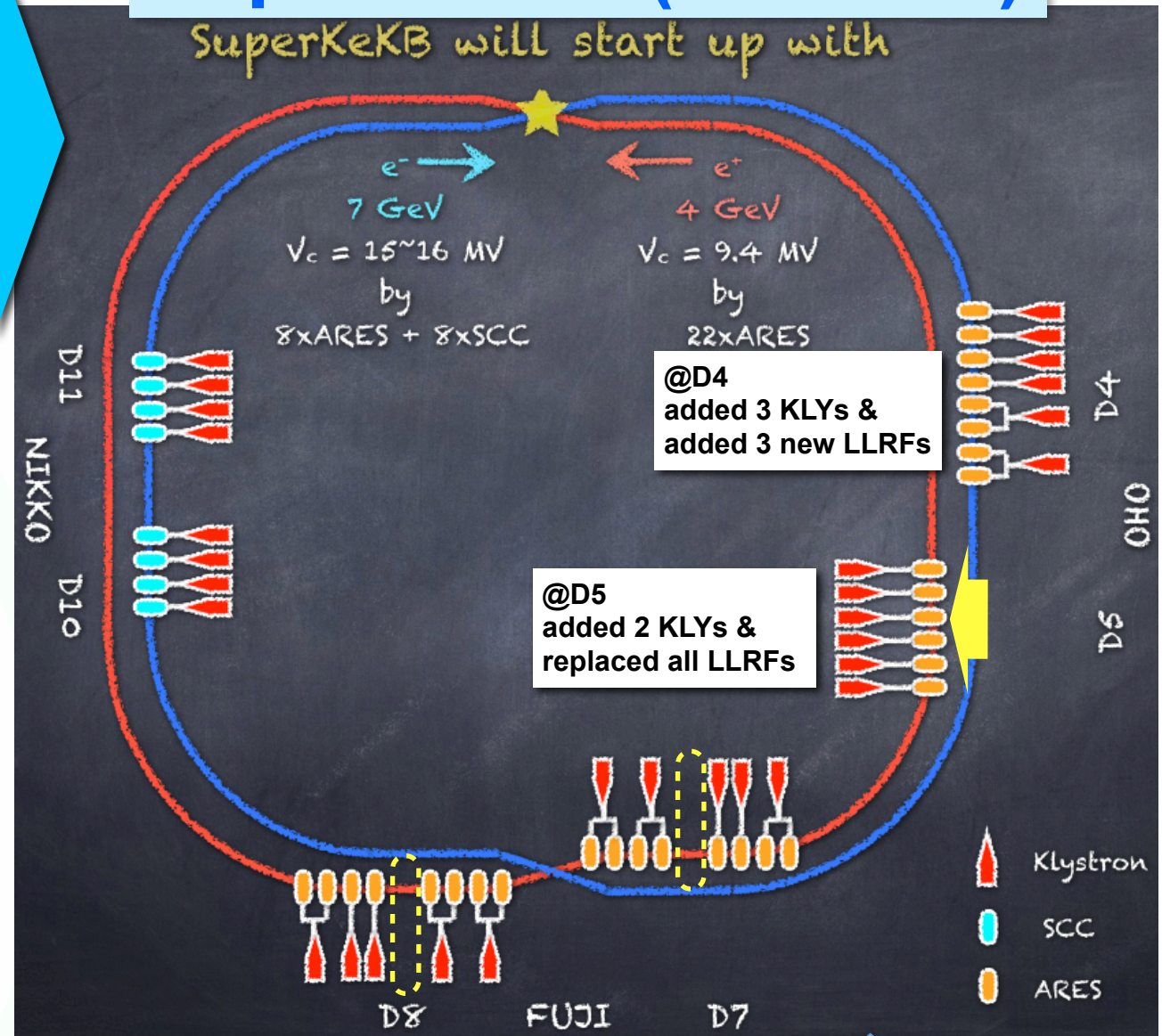
Illustrated by T. Kageyama

Reported '15

## KEKB



## SuperKEKB (Phase 1)



Relocation of ARES cavity from KEBB configuration for Phase-1

- Oho D4: Two cavities were added.
- Oho D5: All six cavities were moved from HER to LER. → 1:1 config.
- Fuji D7: Two cavities were removed.
- Fuji D8: Two cavities were removed.

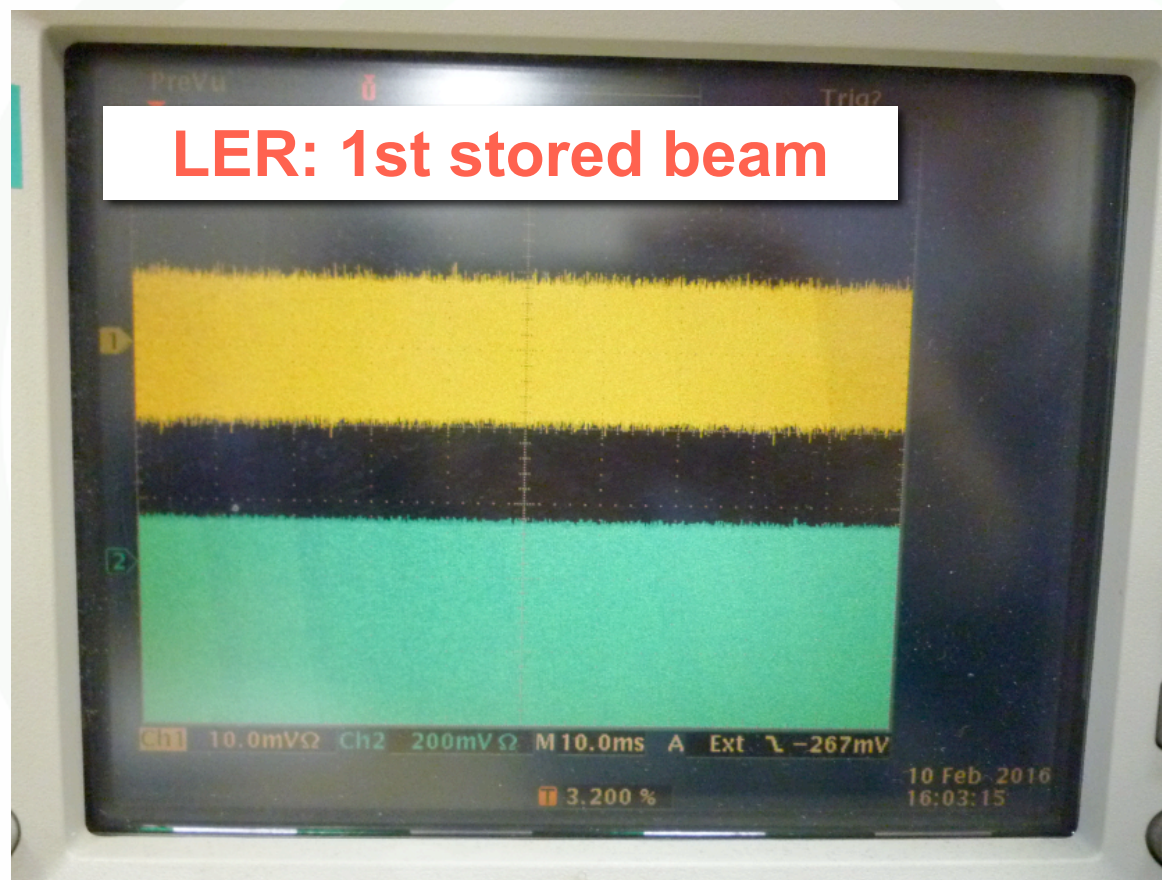


# Successful First Storage by RF-Power On

## After Injection, BT and Optics Tuning

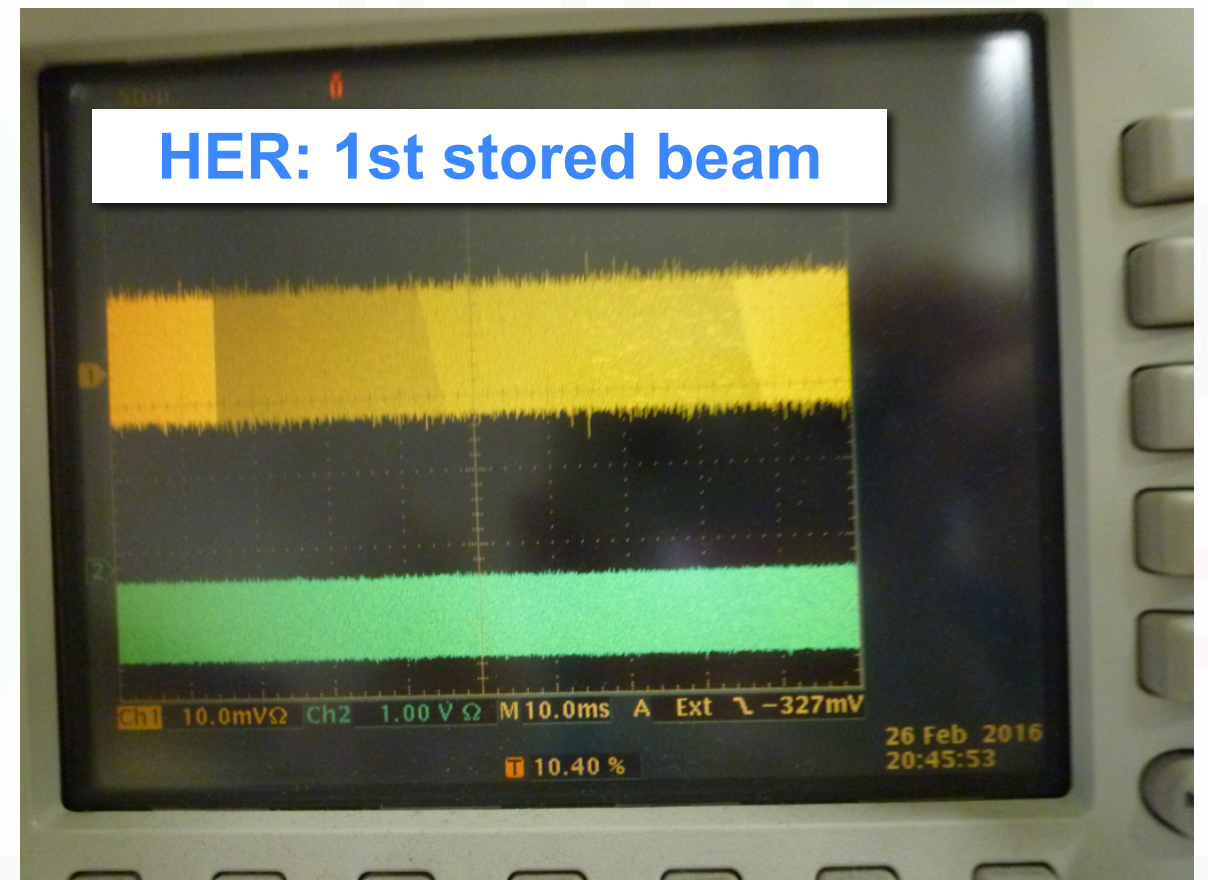
**LER** 10th Feb. 2016

with D7A~E (ARES, D7 all)  
powered-on & RF phase tuning

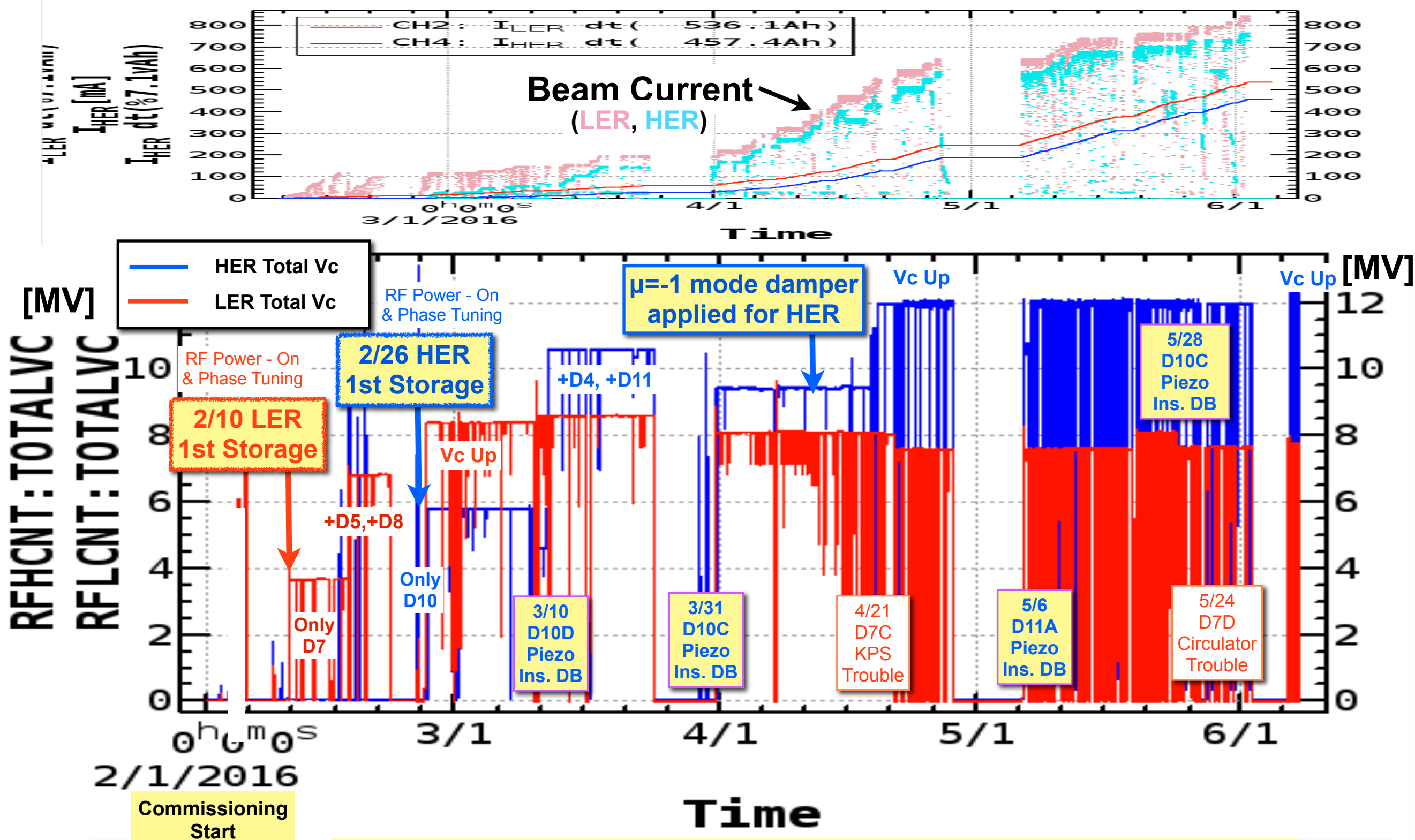


**HER** 26th Feb. 2016

with D10A~D (SCC, D10 All) cavities  
powered-on & RF phase tuning



# History of Ring Acc. Voltage (Total Vc)



RF system has been providing sufficient acc. voltage without critical trouble.

Piezo insulation breakdowns (BD's) occurred frequently in SCC stations. The BD piezo's were replace with a spare, or otherwise, the SC-cavity tuning is controlled by only motorized mechanical tuner without piezo. If no piezo control, the tuning phase stability degrades to be about  $\pm 2$  degrees.

→ Refer Nishiwaki's report for the detail.

# Present Status of RF System

Basically, the RF systems are working well, and very stable now.  
RF trip frequency is enough low in the present stage.

Cav. Trip Rate ARES: ~1 /30 cavs./week  
SCC: <1 /8 cavs./week

State of 06/06 for example

ARES

06/06/2016 23:46:12 Help

Station	L	HV	R	S	RF	SF	IL	FB	Power (kW)	Voltage (MV)	Notes	
D05	A	L	HV	R	S	RF	SF	IL	FB	0. kW	0.01 MV	Saving the electricity cost
	B	L	HV	R	S	RF	SF	IL	FB	0. kW	0.02 MV	
	C	R	HV	R	O	RF	SF	IL	FB	175. kW	0.32 MV	
	D	R	HV	R	O	RF	SF	IL	FB	174. kW	0.32 MV	
	E	R	HV	R	O	RF	SF	IL	FB	160. kW	0.32 MV	
D07	F	R	HV	R	O	RF	SF	IL	FB	155. kW	0.32 MV	
	A	R	HV	R	O	RF	SF	IL	FB	506. kW	0.89 MV	
	B	R	HV	R	O	RF	SF	IL	FB	456. kW	0.89 MV	
	C	R	HV	R	O	RF	SF	IL	FB	220. kW	0.46 MV	
	D	R	HV	R	S	RF	SF	IL	FB	0. kW	0.46 MV	Circulator Water Leak
D08	E	R	HV	R	O	RF	SF	IL	FB	441. kW	0.93 MV	
	A	R	HV	R	O	RF	SF	IL	FB	474. kW	0.96 MV	
	B	R	HV	R	O	RF	SF	IL	FB	550. kW	0.93 MV	
	C	R	HV	R	O	RF	SF	IL	FB	245. kW	0.45 MV	
	D	R	HV	R	S	RF	SF	IL	FB	0. kW	0.45 MV	Cav. Vacuum Trouble
E	R	HV	R	O	RF	SF	IL	FB	493. kW	0.91 MV		

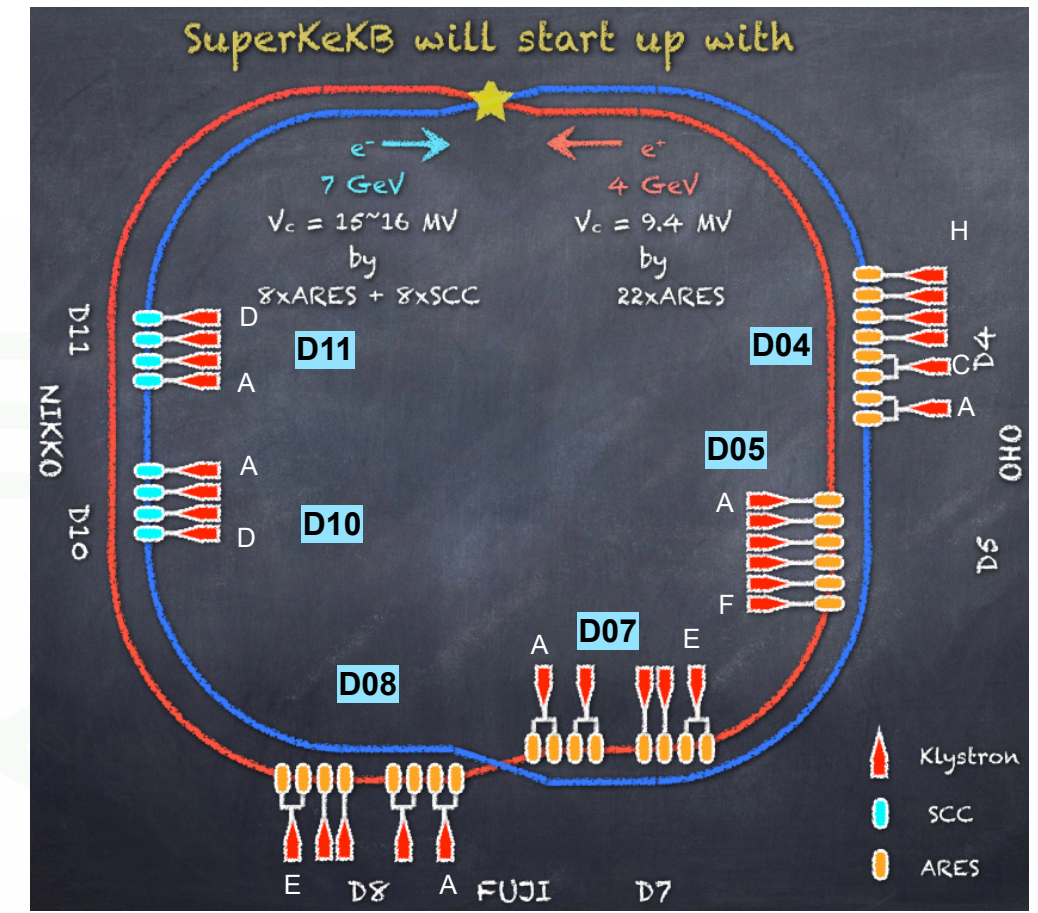
**LER**  
LER Vc  
7.78 MV  
Beam  
829.6 mA  
↓  
910mA

Station	L	HV	R	S	RF	SF	IL	FB	Power (kW)	Voltage (MV)	Notes	
D04	A	R	HV	R	O	RF	SF	IL	FB	367. kW	0.76 MV	
	C	R	HV	R	O	RF	SF	IL	FB	347. kW	0.71 MV	
	E	R	HV	R	O	RF	SF	IL	FB	177. kW	0.35 MV	
	F	R	HV	R	O	RF	SF	IL	FB	198. kW	0.33 MV	
	G	R	HV	R	O	RF	SF	IL	FB	213. kW	0.34 MV	
D10	H	R	HV	R	O	RF	SF	IL	FB	246. kW	0.34 MV	
	A	R	HV	R	S	RF	SF	IL	FB	0. kW	1.36 MV	Piezo Break Down → Recovered
	B	R	HV	R	O	RF	SF	IL	FB	210. kW	1.36 MV	
	C	R	HV	R	O	RF	SF	IL	FB	207. kW	1.34 MV	
	D	R	HV	R	O	RF	SF	IL	FB	227. kW	1.34 MV	
D11	A	R	HV	R	O	RF	SF	IL	FB	229. kW	1.36 MV	
	B	R	HV	R	O	RF	SF	IL	FB	219. kW	1.36 MV	
	C	R	HV	R	O	RF	SF	IL	FB	196. kW	1.35 MV	
	D	R	HV	R	O	RF	SF	IL	FB	219. kW	1.35 MV	

**HER**  
HER Vc  
12.37 MV  
Beam  
754.3 mA  
↓  
830mA

SCC

RingRFCATV07 on localhost:12.0



In the several stations (D5A,D5B, D7D, D8D, D10A), the cavities are powered-off and detuned to put out of operation for some reasons.

Present state, D10A is recovered without piezo control.

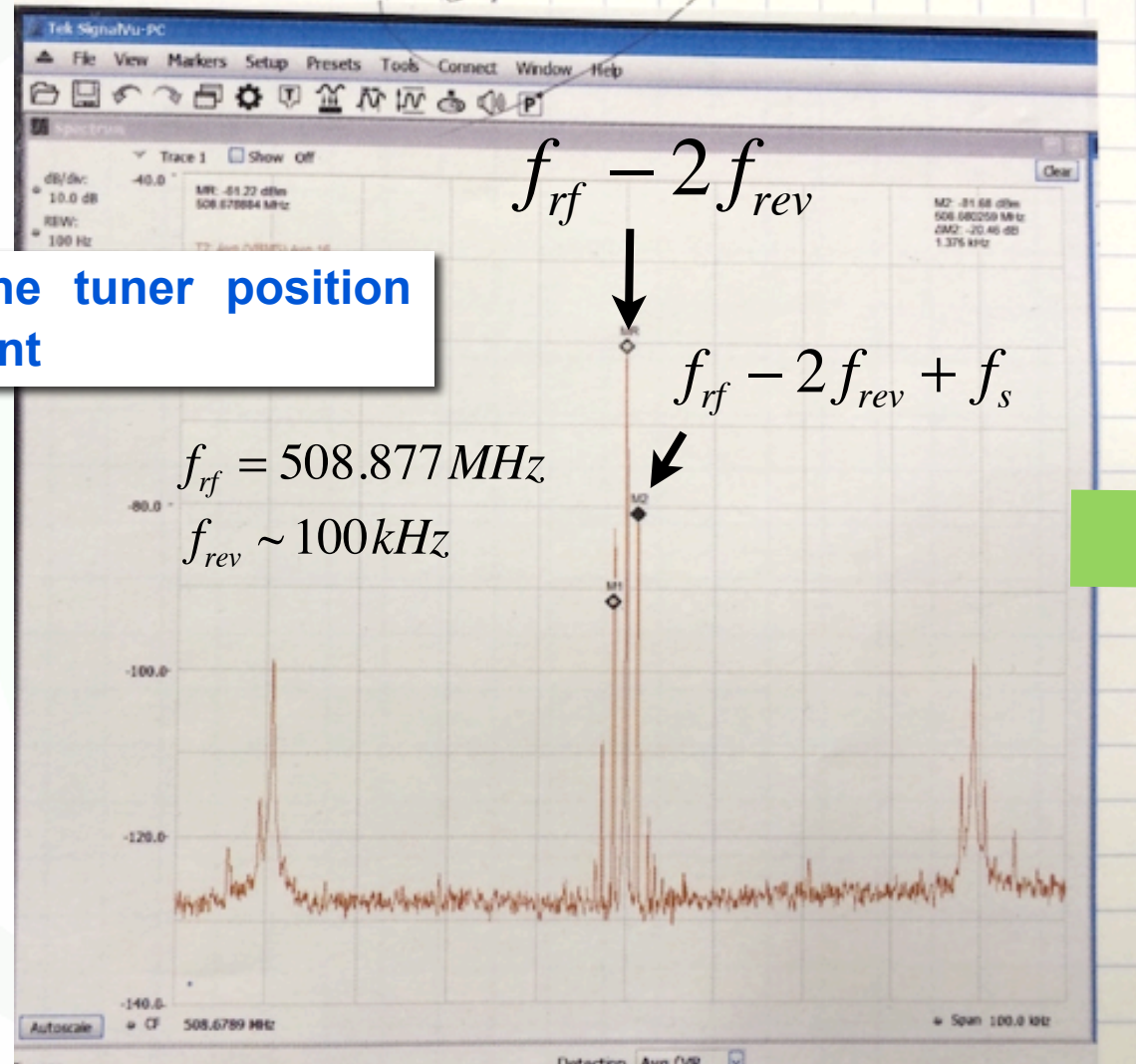
Operation power of the klystron is still far from the saturation. There is enough margin in the klystron performance.

# $\mu=-1$ & $-2$ Mode Osc. due to Detuned Cavity (Power-off)

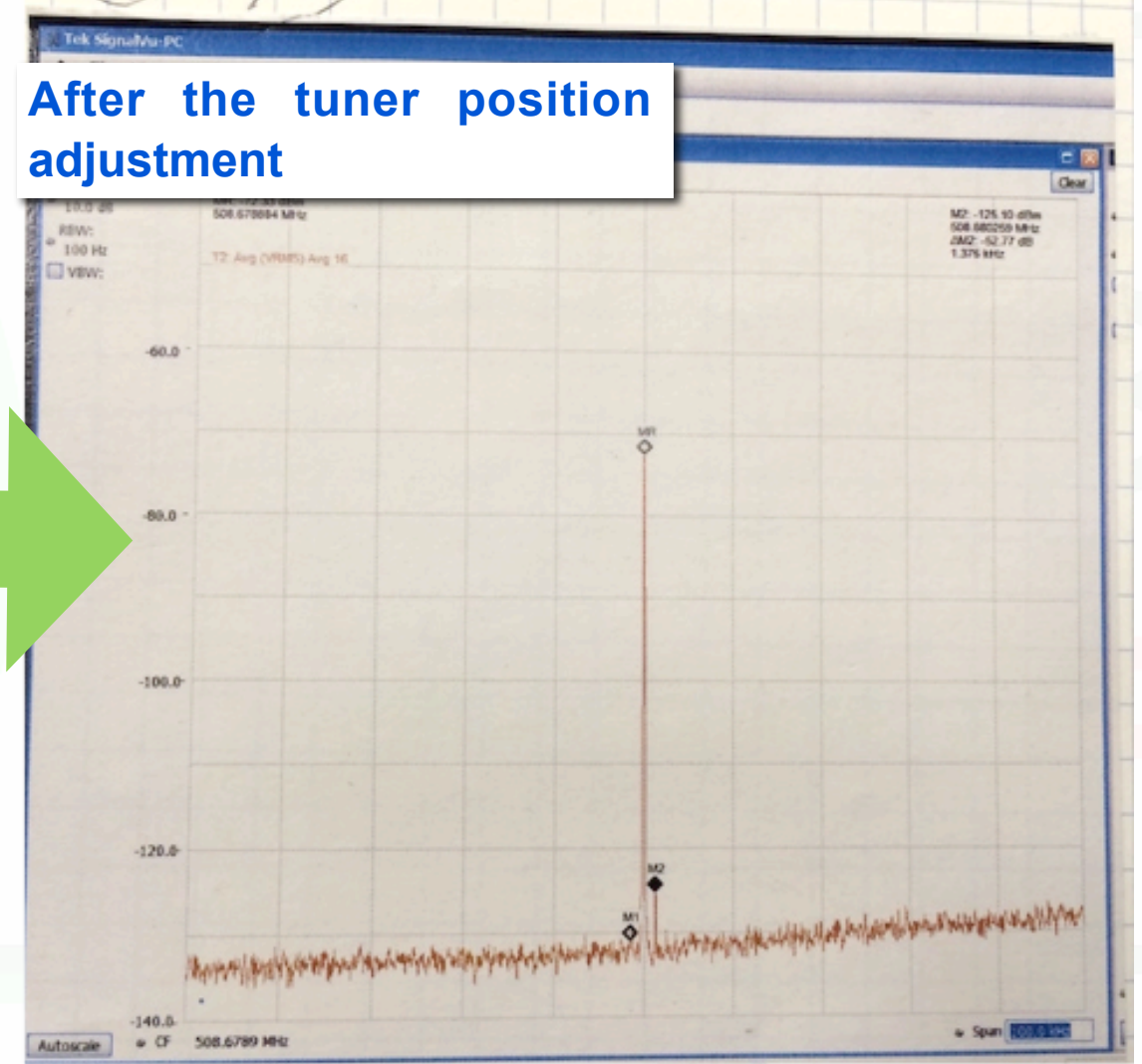
Even though the beam current was low, coupled bunch instability (longitudinal bunch oscillation) of the  $\mu=-1$  or  $-2$  mode was occasionally induced by the detuned cavities (both of ARES and SCC), which were powered-off and put out of the operation because of trouble or saving cost, In that case, the tuner position of the detuned cavity had to be adjusted to reduce the instability.

## Example of $\mu=-2$ mode instability by a detuned ARES Cavity

Before the tuner position adjustment



After the tuner position adjustment



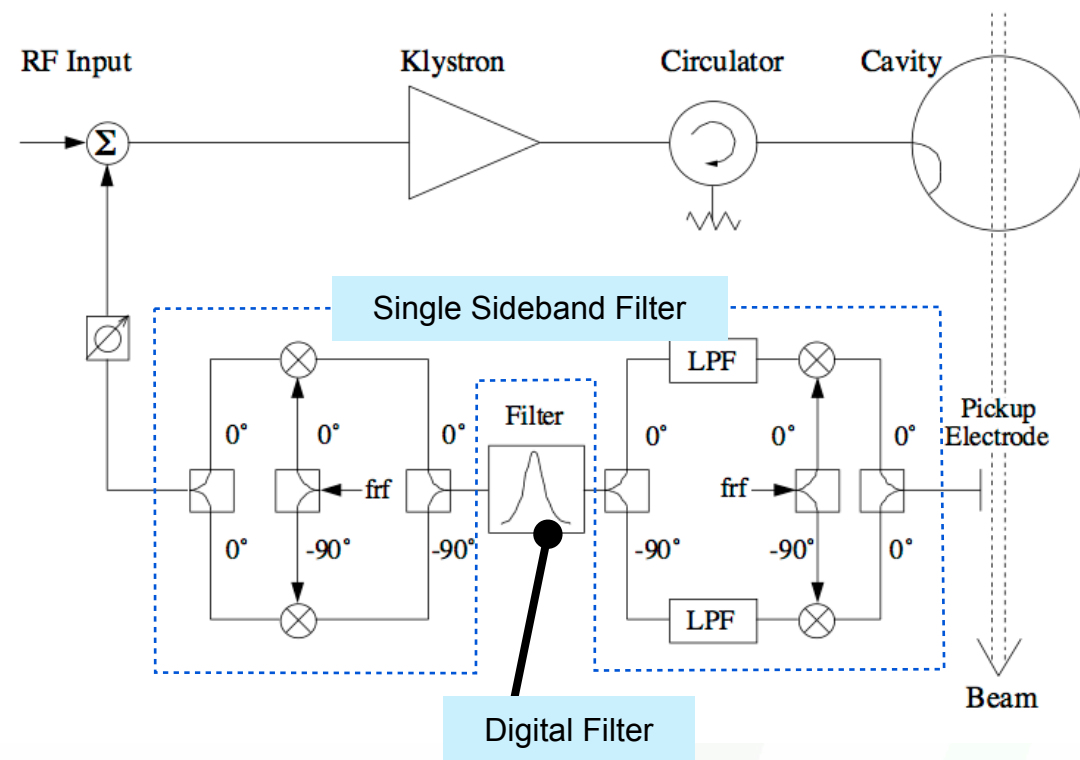
# The $\mu=-1$ Mode Damper Applied for HER

In HER, over the 470-mA beam current, the  $\mu=-1$  mode instability due to the detuned (troubled) cavities could not be suppressed by the tuner adjustment. Consequently, the  $-1$  mode damper system, which had been used in KEKB operation, was applied to the D4 station. It worked well to suppress the  $\mu=-1$  mode successfully and the beam current could be increased.

Predicted threshold current of the  $\mu=-1$  mode instability due to the acc. mode :  $\sim 1.1\text{A}$  (HER)  
 $\sim 1.6\text{A}$  (LER)

At an earlier stage than expected, the  $\mu=-1$  mode damper became required.

## Block diagram of the $-1$ Mode Damping System



The  $\mu=-1$  mode digital feedback selectively reduces impedance at the driving frequency.

## For the $\mu-2$ mode,

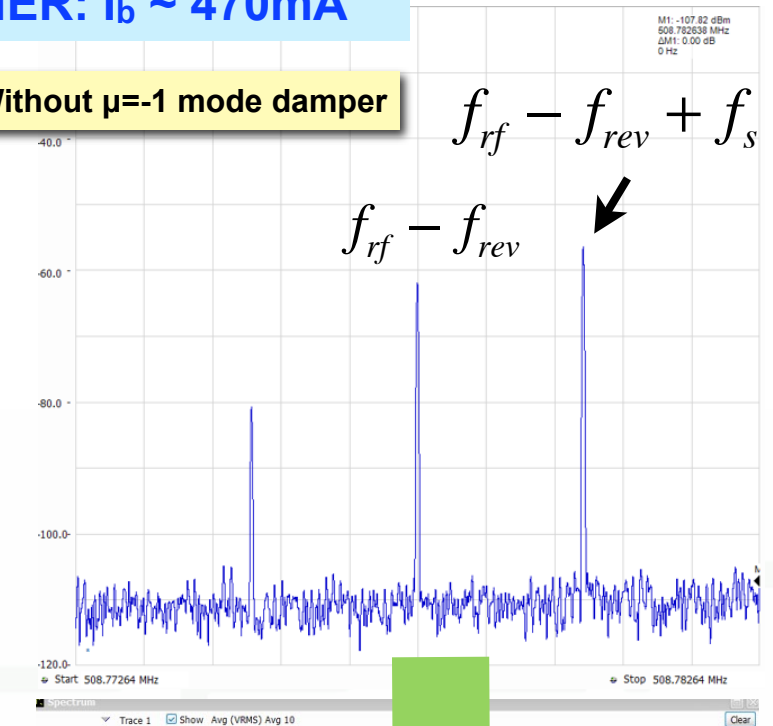
The predicted threshold current of the  $\mu=-2$  mode instability due to the acc. mode is near the design current value of SuperKEKB (Ref. the 16th review committee). Therefore, the  $\mu=-2$  mode damper system is necessary for Phase-2.

New digital feed back system of the  $\mu=-2$  mode damper is now under development for Phase-2. It will be also available for the  $\mu=-3$  mode.

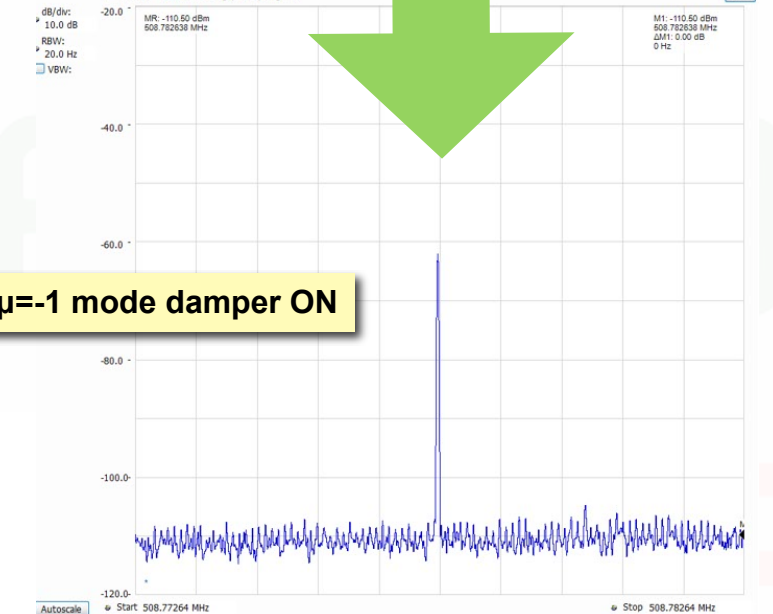
The  $\mu=-2$  and  $-3$  mode damper is no less required for the suppression of the instability due to the detuned (power-off) cavities.

HER:  $I_b \sim 470\text{mA}$

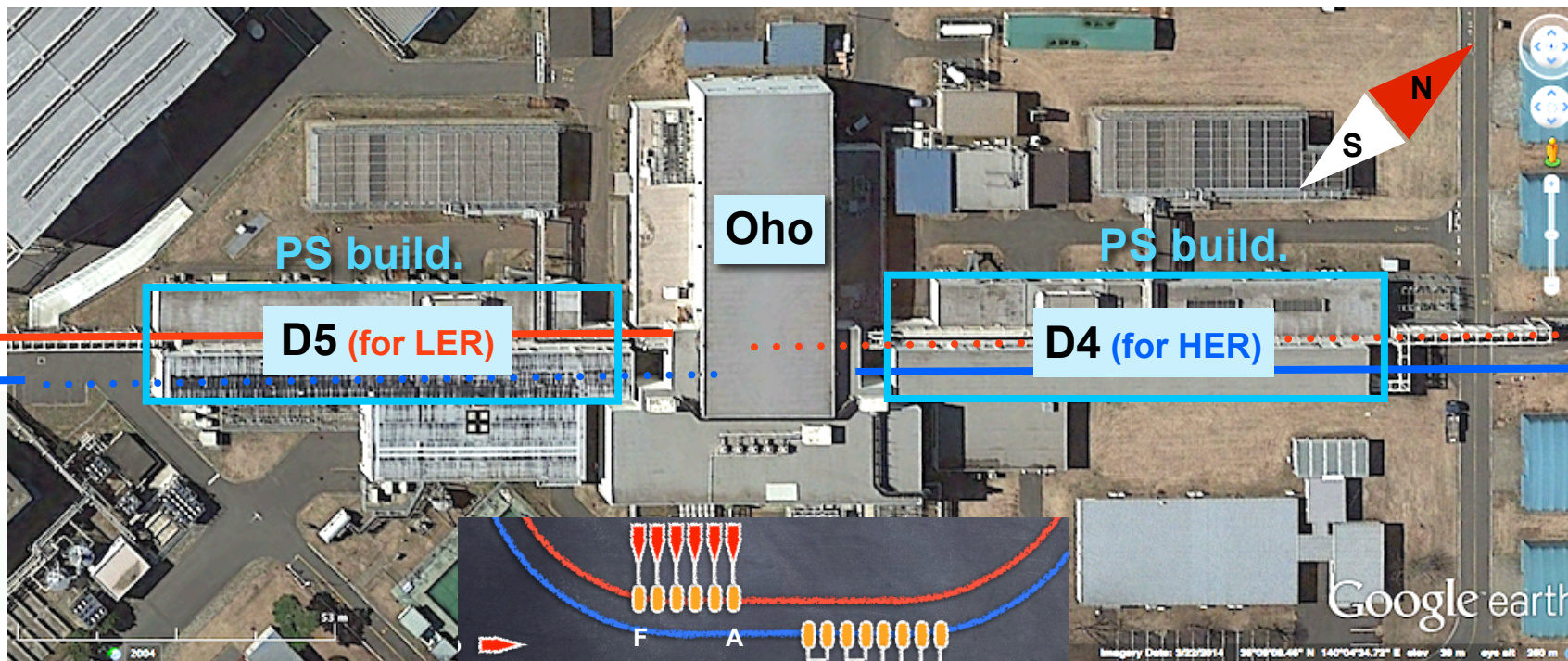
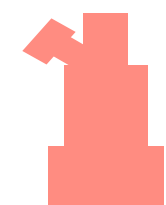
Without  $\mu=-1$  mode damper



$\mu=-1$  mode damper ON



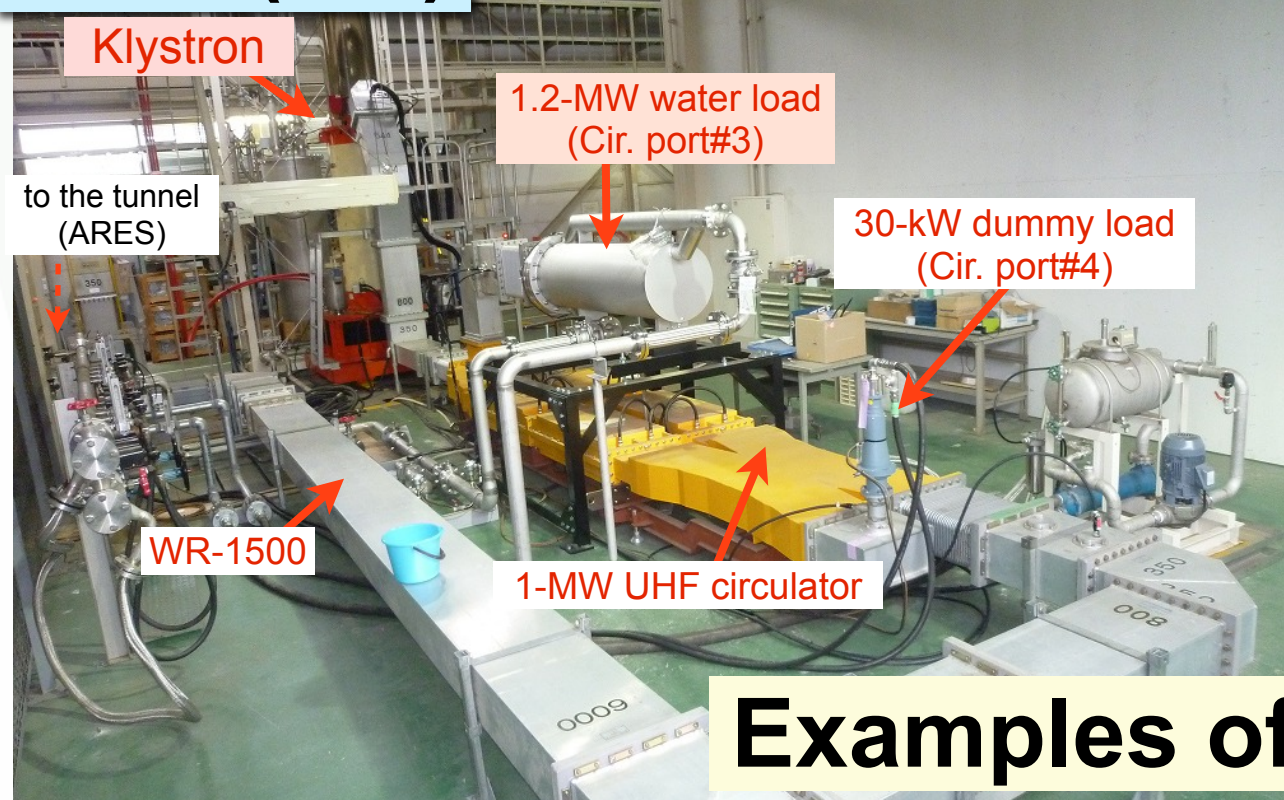
# High Power RF System (above-ground part)



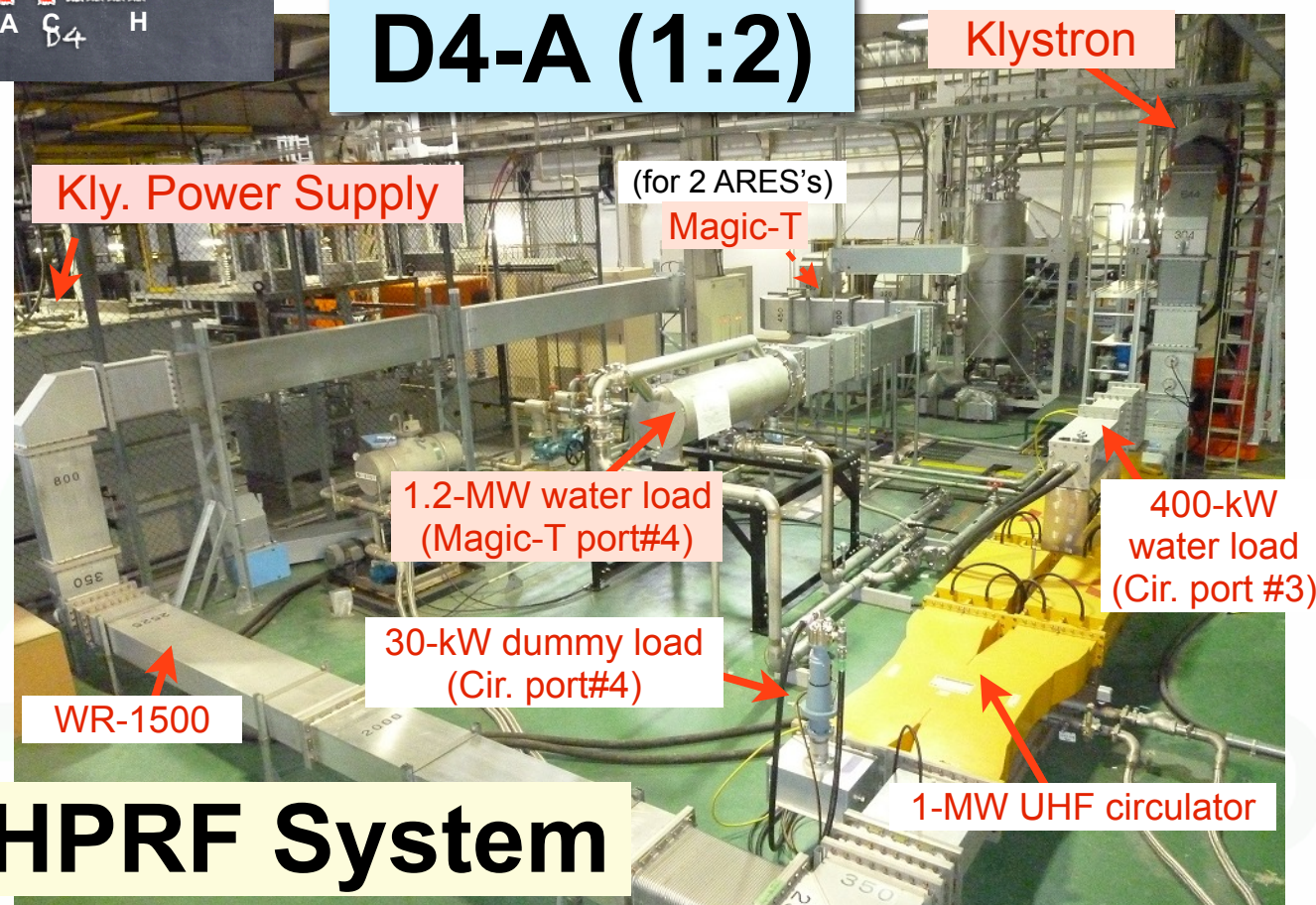
to Fuji  
+e

to IP  
-e

## D5-F (1:1)



## D4-A (1:2)



## Examples of HPRF System

Many components used in TRISTAN operation were reused. Regular maintenance of them is needed.

# Status of High Power RF System



## ▶ Klystron

- 30 Klystrons are operated smoothly without troubles.

## ▶ Klystron Power Supply (KPS)

- The KPSs are also operated without serious trouble

## ▶ High-power components (Waveguides, circulators and dummy loads)

- The high power components are enough sound and stable without big troubles except for the circulator water leak at D7D station.

## ▶ Cooling systems (for the Klystrons and the dummy loads)

- Water leak troubles are happened due to the aging degradation of components. (\*\*Many components of the cooling systems have been used since the TRISTAN operation. \*\*)
- These components will be changed to new one or repaired as soon as possible when the water leak is found.

Klystron Cooling System



Air Cooled Heat Exchanger



# DR Status of HPRF System



The construction of high-power RF system for DR was started from October 2015.  
The high power test without cavity is scheduled in winter 2016.

## ▶ Klystron

- Klystron setup : finished. Fig. a  
(It was moved from D11-E to DR at Jan 2016)

## ▶ Klystron Power Supply (KPS)

- Type-B KPS setup: finished. Fig. a  
(It was moved from D4 to DR at Dec 2015,  
and the control console for KPS was renewed to new one.)

## ▶ High Power Components

- Connection of waveguide system: finished. Fig. a, b
- Construction of a stage for vapor cooling system: finished. Fig. c

## ▶ Current Works for the High Power Test (Winter 2016)

- Construction of the vapor cooling system.
- Installation of the water cooling pipes.
- Wiring of the power and control cables.

Details about DR cavity system are presented by T. Abe.

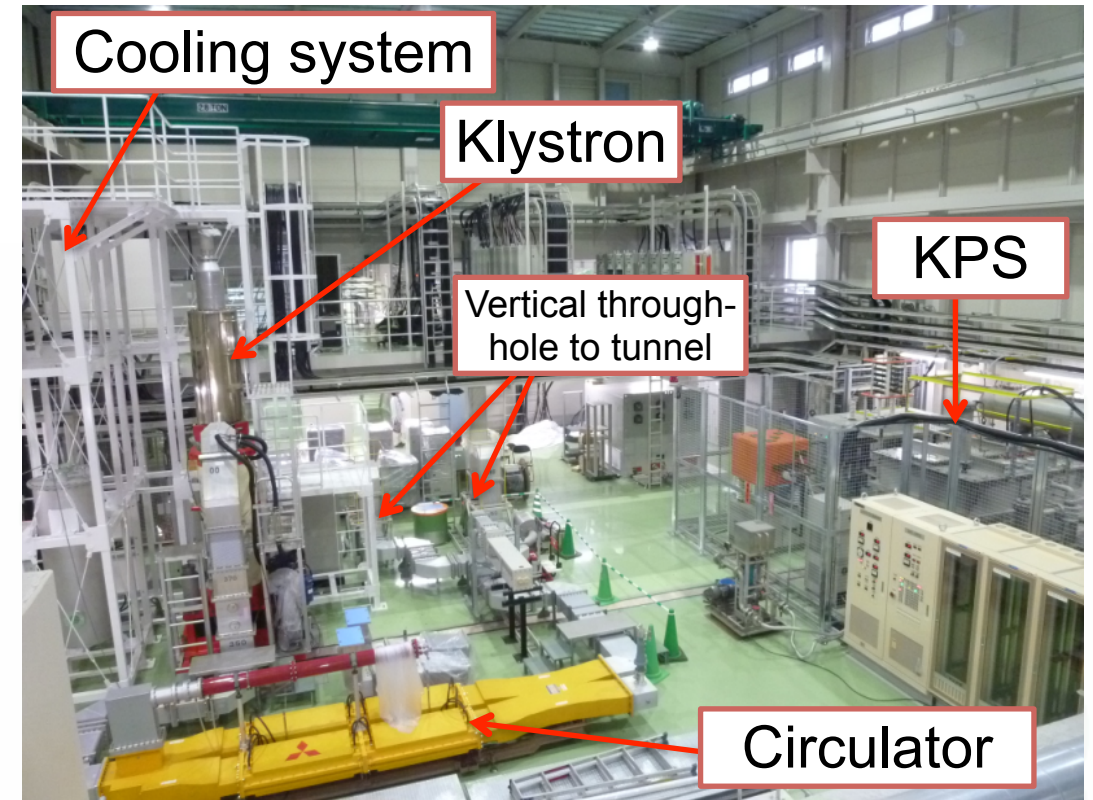


Fig. a



Fig. b

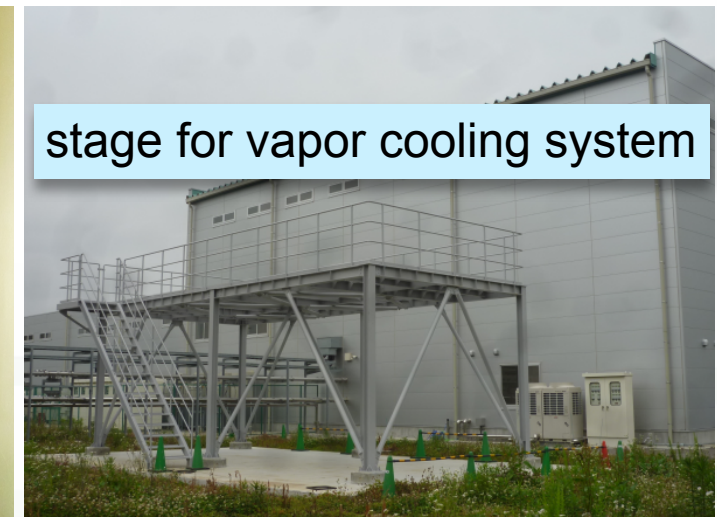
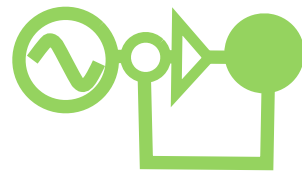


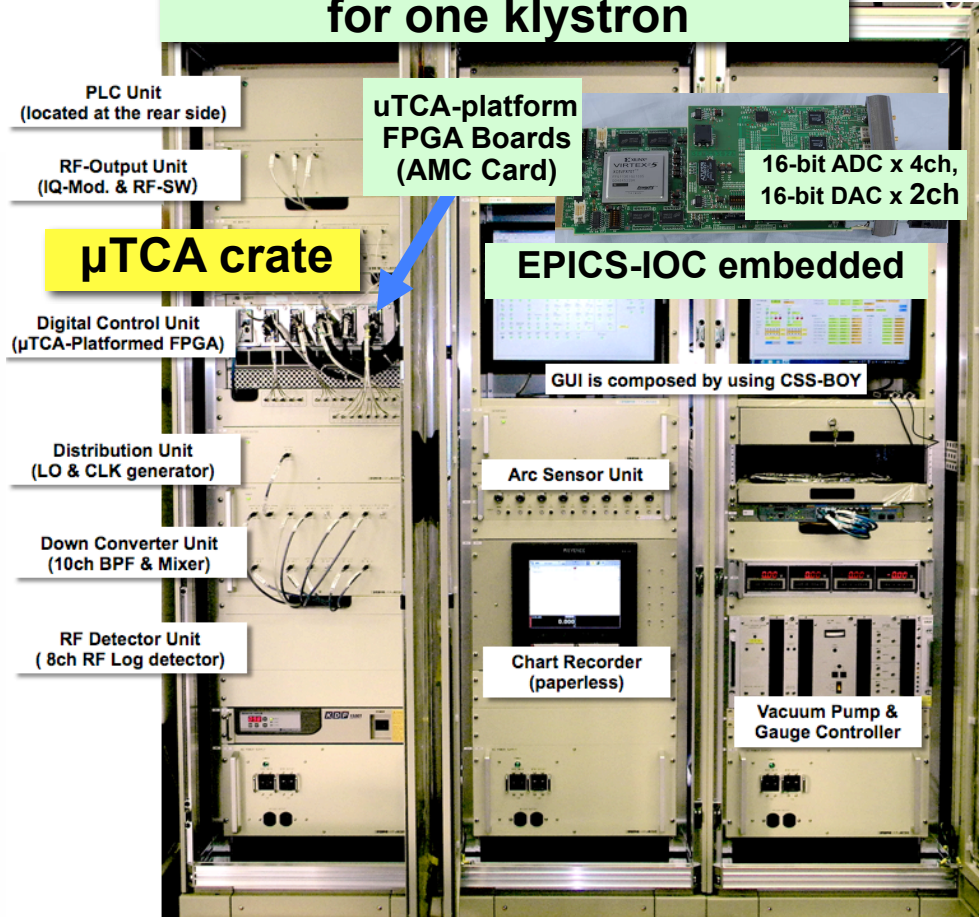
Fig. c

# New LLRF Control System



was developed for higher accuracy and flexibility for SuperKEKB.

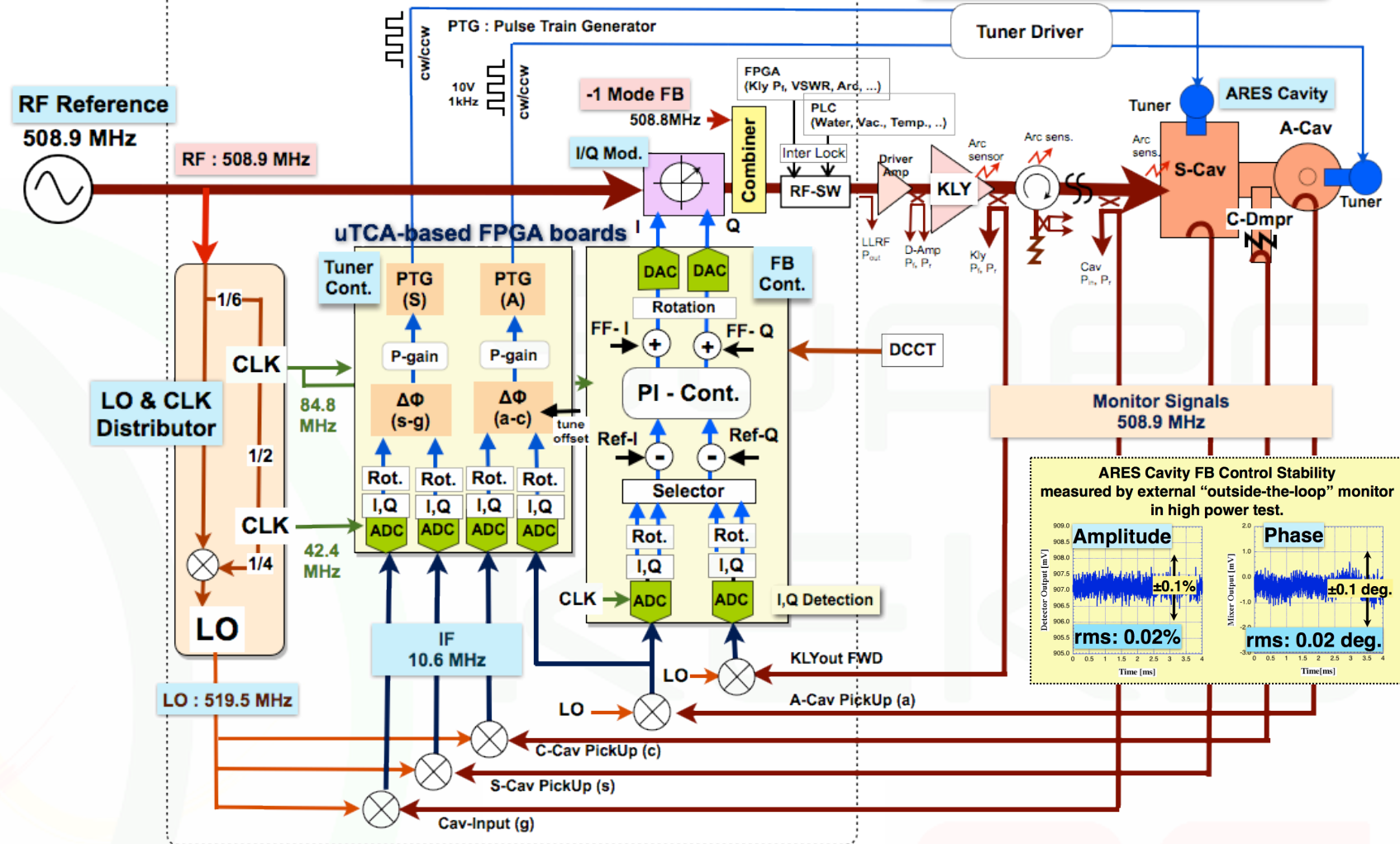
## New LLRF System for one klystron



- Consisting of μTCA-platformed FPGA boards (AMC), & PLC.
- EPICS-IOC with Linux-OS is embedded in each of them.
- Common hardware for both of ARES & Superconducting Cavity.
- Klystrons (LLRF) : Cavity unit = 1 : 1 (SuperKEKB)

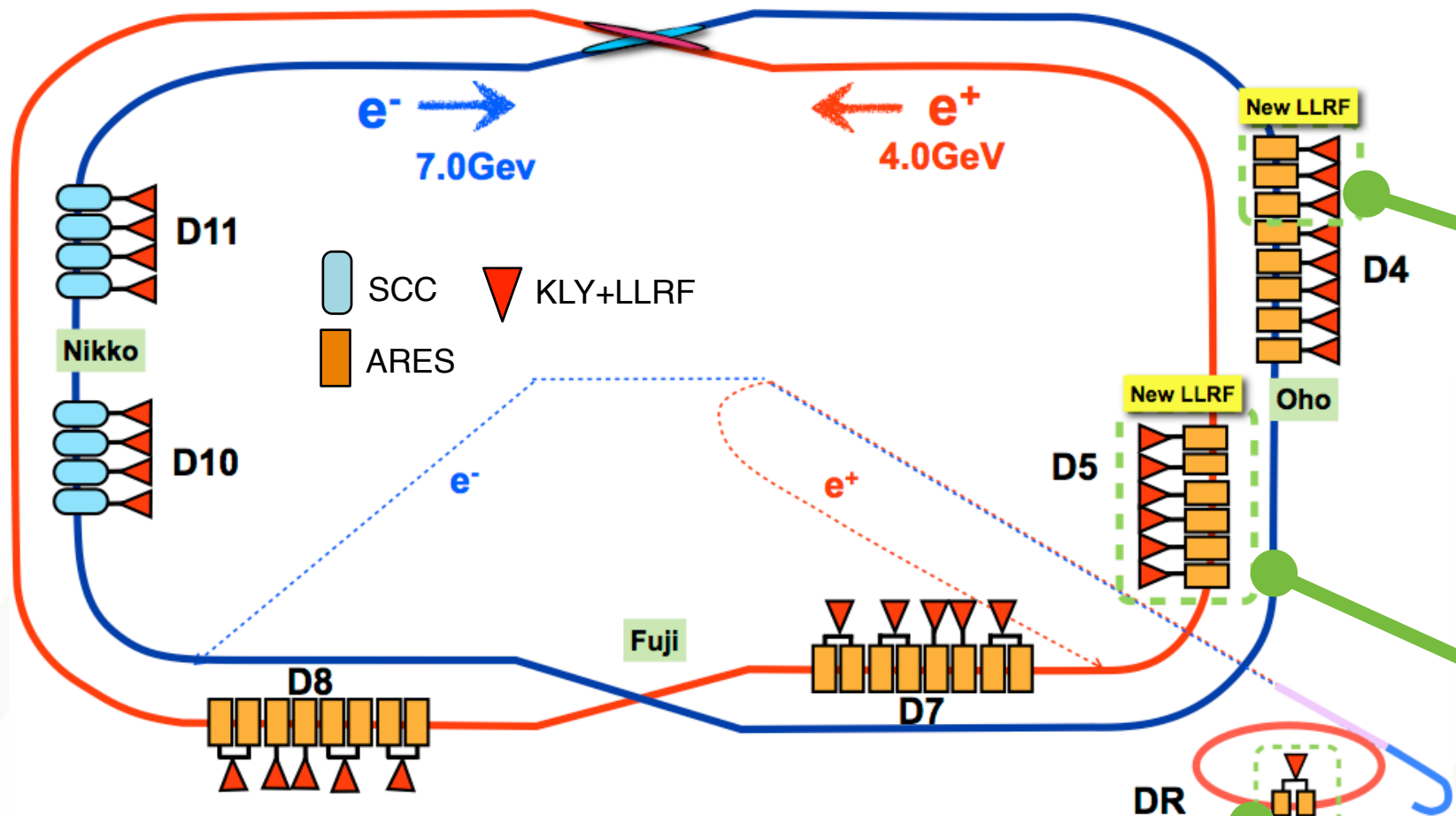
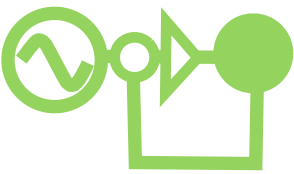
**Completely remote controllable**

## LLRF System



- New LLRF control system is built on recent digital technique. It is dominated by μTCA-platformed FPGA boards for higher accuracy and flexibility.
- In this system, I/Q components are handled by FPGA for vector control instead of amplitude and phase.
- The good performance was demonstrated in the high power test with ARES cavity., The regulation stability was 0.02% in amplitude and 0.02 deg. in phase.

# Status of new LLRF System



@OHO D4 Control Room

Old systems



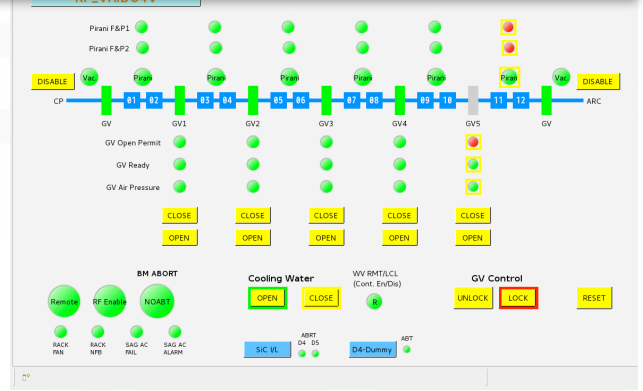
**3 new LLRF systems**

@OHO D5 Control Room



**6 new LLRF systems**

Integrated Vacuum control system

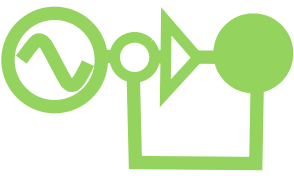


@DR Control Room

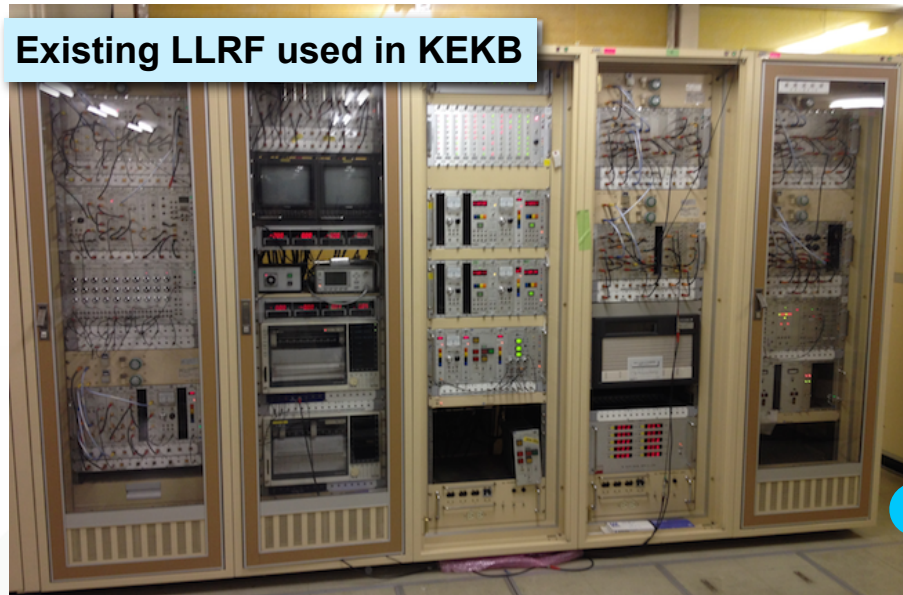
## Status

- At 9 stations of Oho D4&D5 (6@D5 + 3@D4), the LLRF control systems were replaced with new digital control systems.
- Vacuum gate-valve control-integration system at OHO RF section is also upgraded to make matching with the new digital LLRF systems for flexibility and convenience. Details are presented by M. Nishiwaki.
- All of new systems are successfully working well without problem. Some software bugs found during the operation were fixed.
- The DR-LLRF control system has already installed in DR control room. It is almost the same as MR one, except 3-cavity vector-sum control is needed. In the present stage, the number of cavities is two.

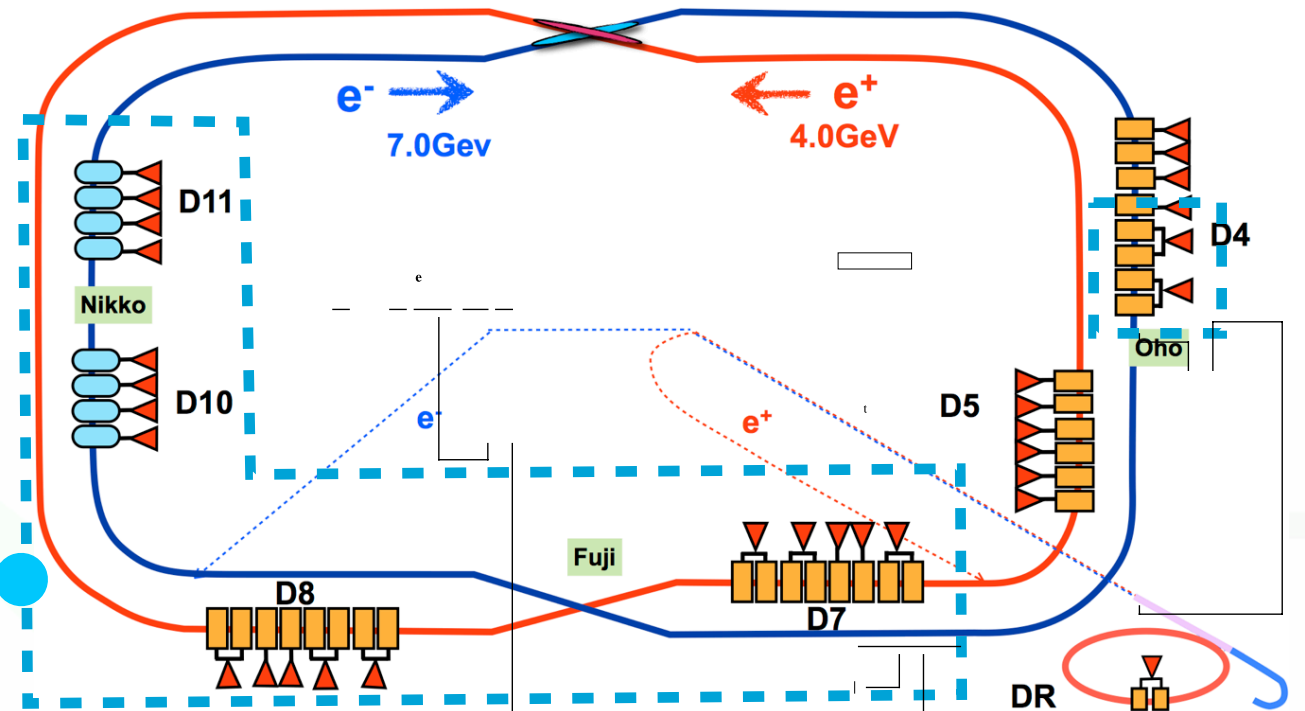
# Existing Analog LLRF System



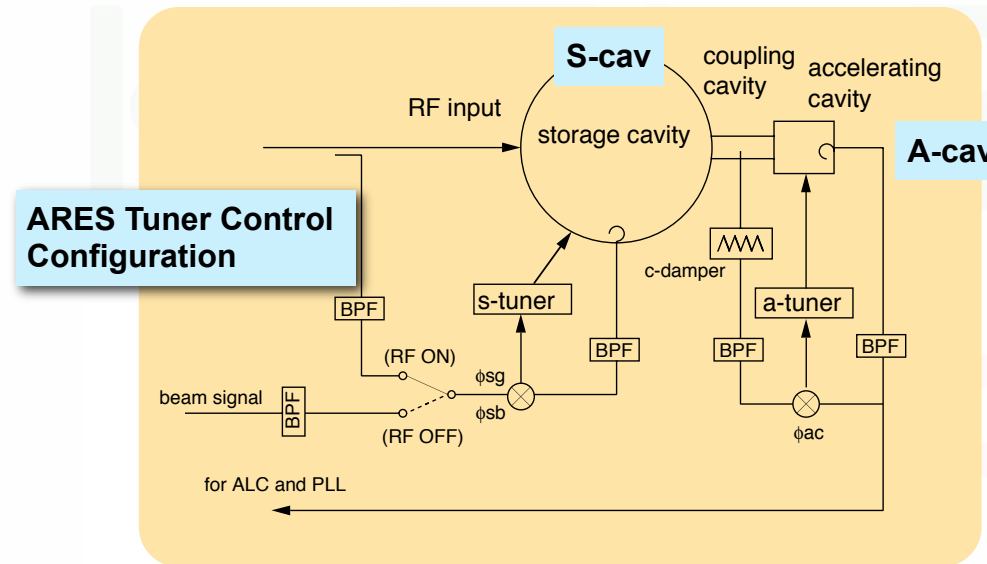
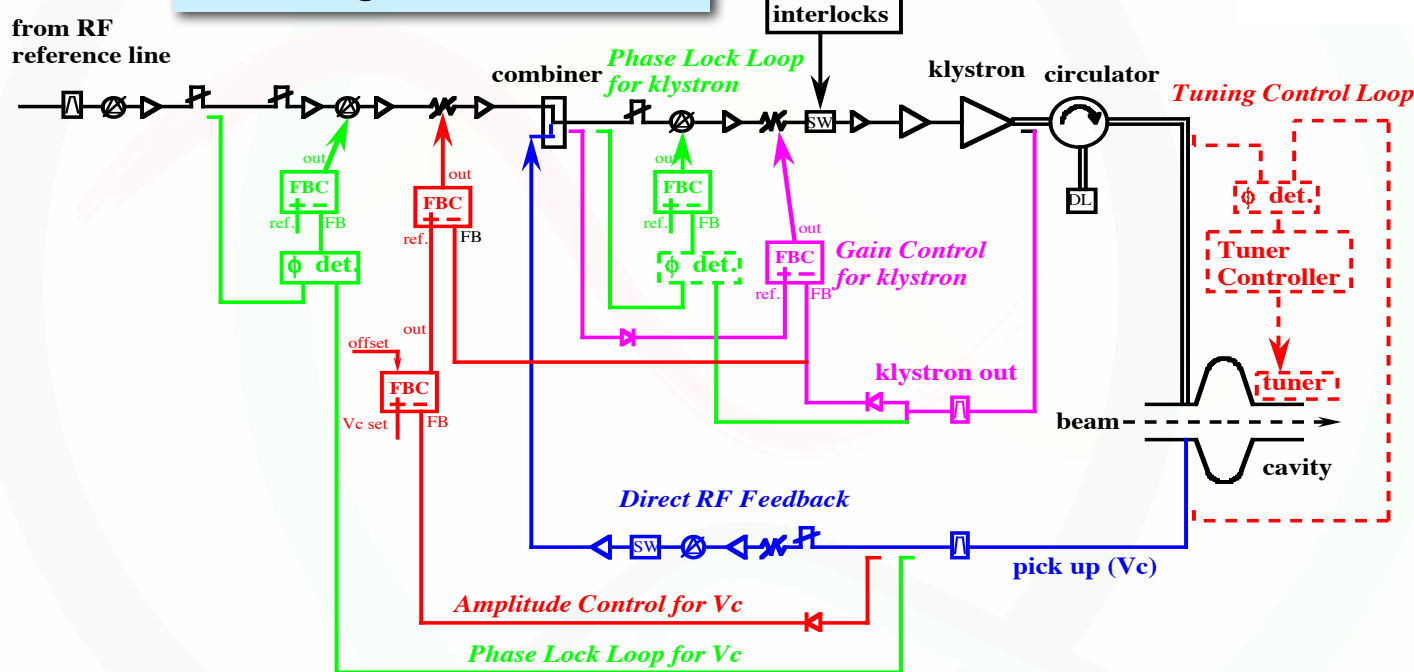
Most stations are still operated by existing old LLRF systems, which had been used in KEKB operation



Existing LLRF used in KEKB

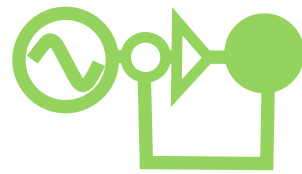


Block Diagram of SCC LLRF



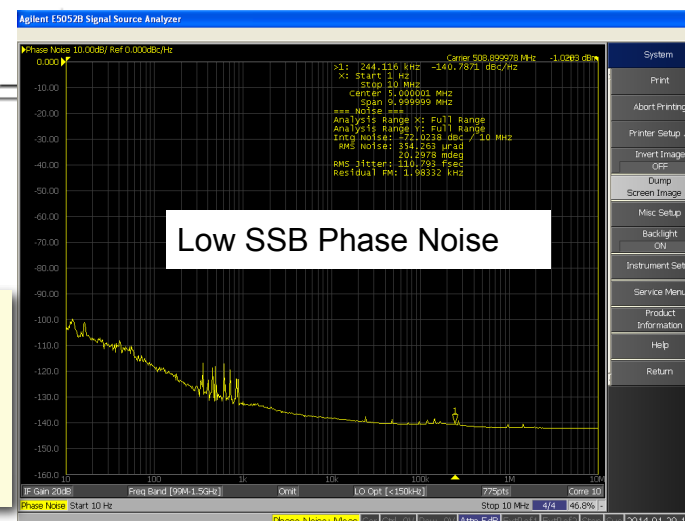
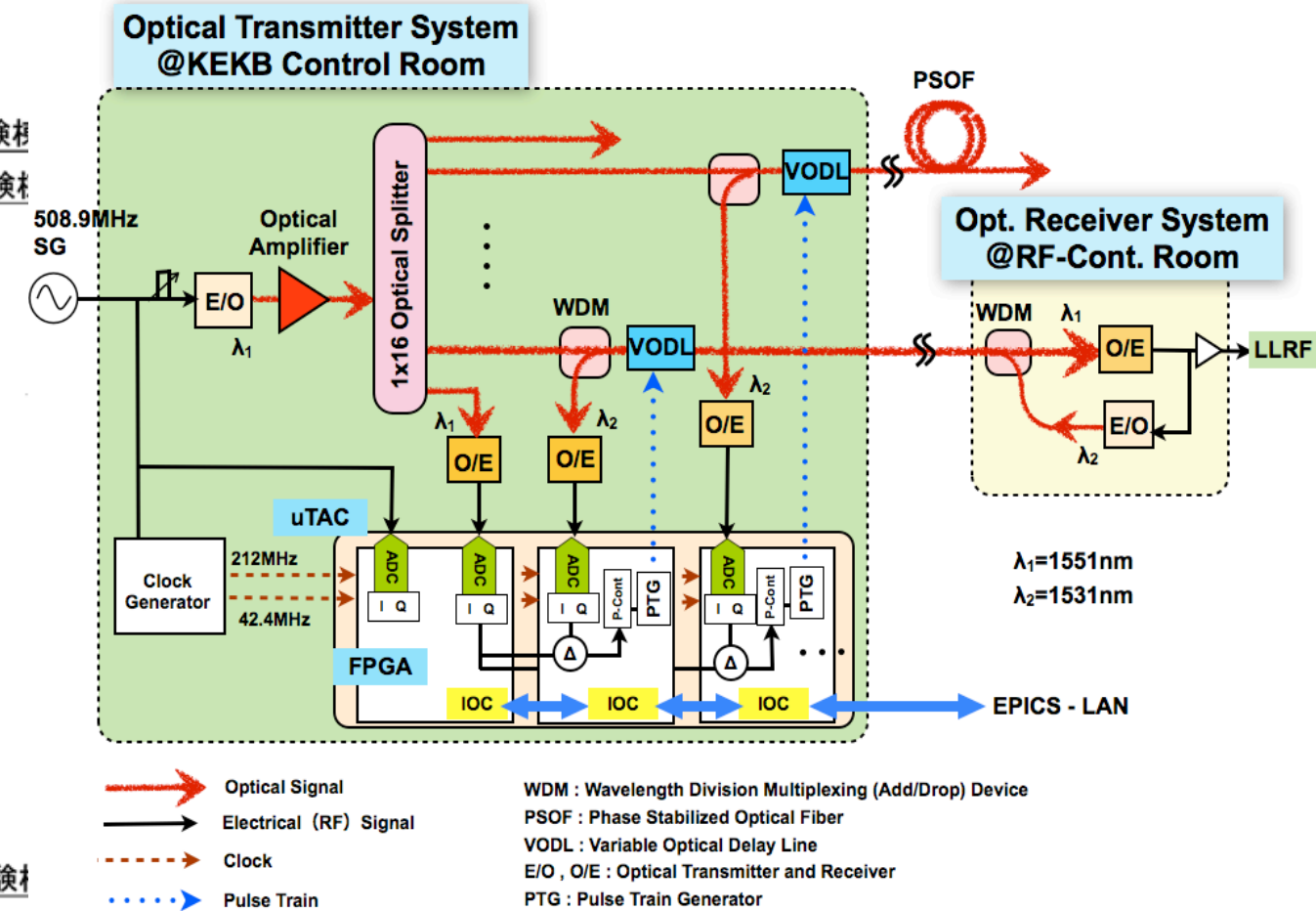
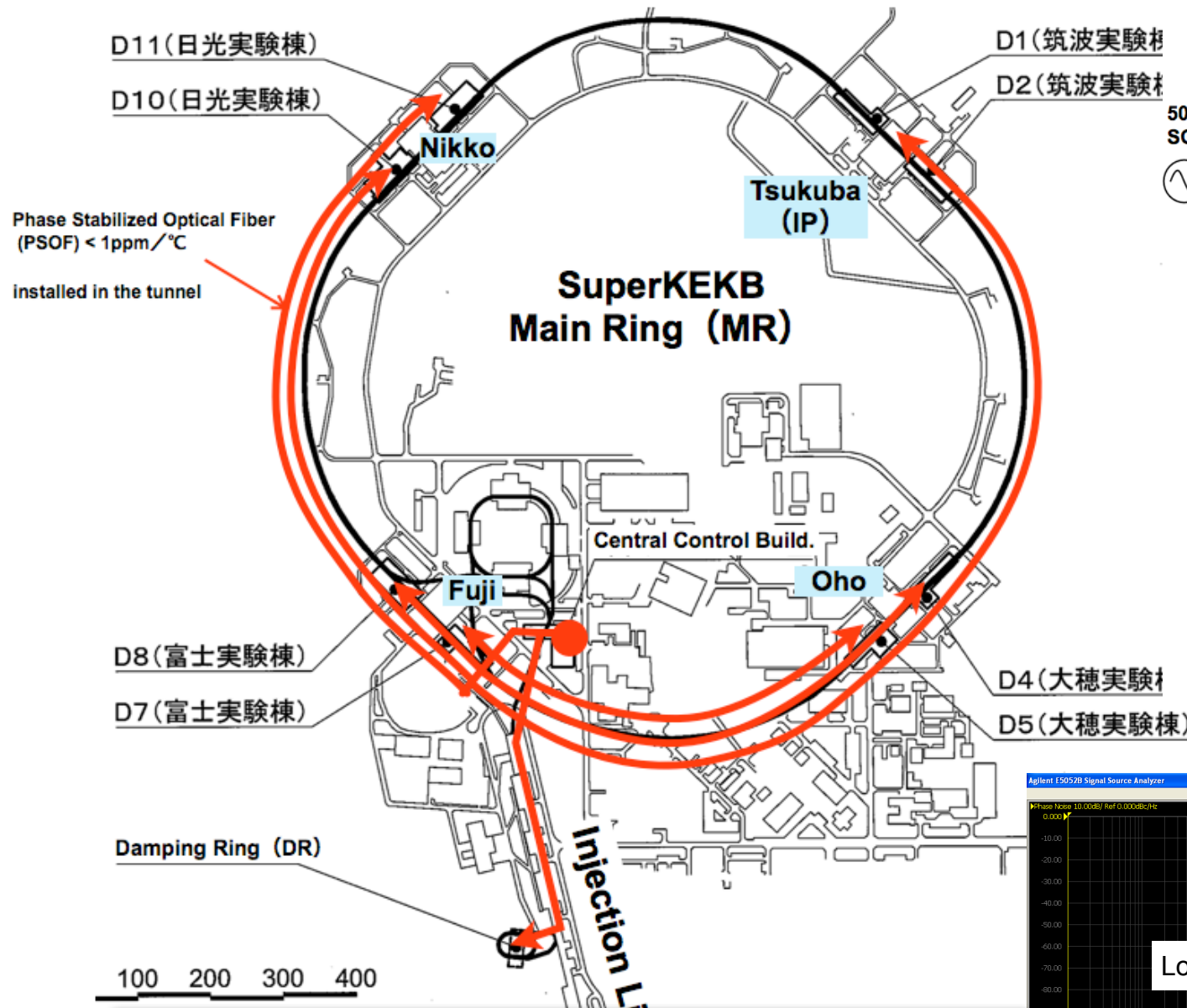
- These systems are composed of combination of NIM standard analogue modules.
- They are controlled remotely via CAMAC system.
- All systems are soundly working as well as operated in the KEKB operation without serious troubles, however, many old defective modules were replaced with spares in the maintenance works.

# RF Reference Distribution



with digital optical delay control for phase stabilization

- RF reference signal is optically distributed into 8 sections by means of “Star” topology configuration from the central control room (CCR).
- “Phase Stabilized Optical Fiber”, which has quite small thermal coefficient, is adapted :  $< 1\text{ppm}/^\circ\text{C}$
- For the thermal phase drift compensation, optical delay line is controlled digitally at CCR for all transfer lines.
- The phase noise (time jitter) is enough low.



Variable Optical Delay Lines (VODLs) for 8 transmissions

uTCA-platformed FPGAs for the VODLs control



Short term stability (time jitter) :  $\sim 0.1\text{ ps (rms)}$

Long term stability (pk-pk) :  $\pm 0.1^\circ @ 508.9\text{MHz} = \pm 0.55\text{ ps}$  (expected by the optical delay control)

# Bunch Gap Transient Effect on Beam Phase

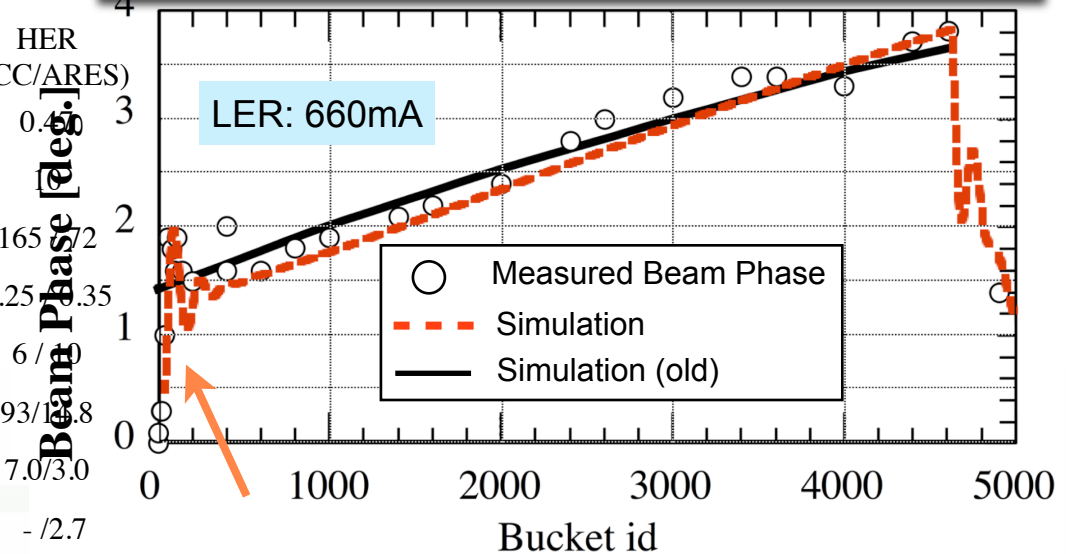
[T. Kobayashi and K. Akai, Phys. Rev. Accel. Beams 19, 062001 \(2016\)](#)

Published 9 June 2016

# Simulation of Bunch Gap Transient Effect

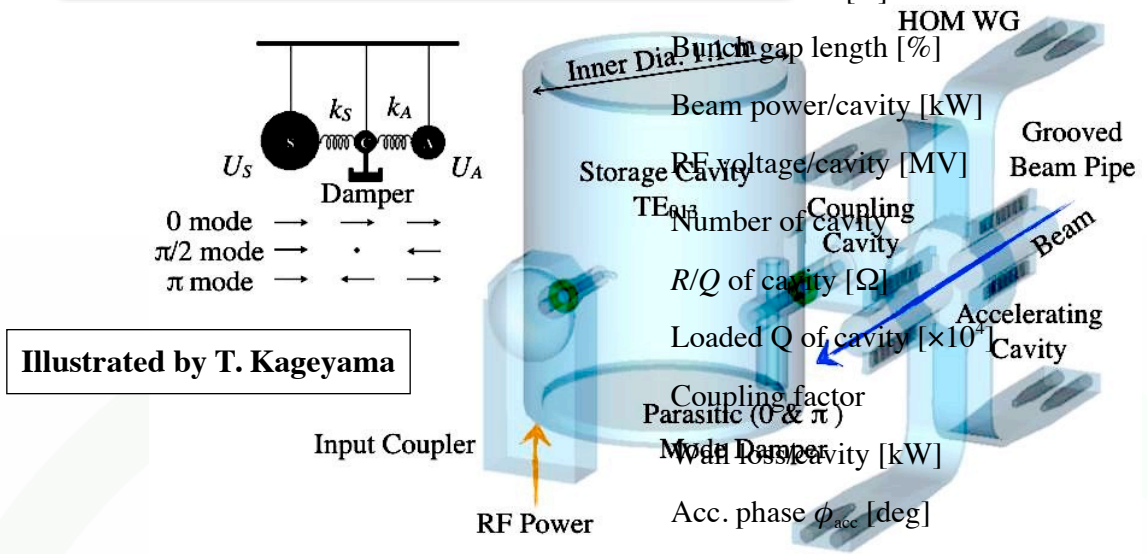
New time domain simulation code was created to estimate the transient loading in ARES. This simulation can calculate the RF time evolution of the three-cavity system of ARES.

Observed beam phase in KEKB operation



With including the three-cavity structure of ARES in the calculation, the rapid phase change at the leading part of the bunch train can be reproduced by the simulation. It was clarified that the rapid phase change is attributed to the parasitic (0&pi) mode of ARES.

ARES Cavity (3-Cav. System)



Illustrated by T. Kageyama

$$\begin{bmatrix} V_{ar}^{n+1} \\ V_{aj}^{n+1} \\ V_{cr}^{n+1} \\ V_{cj}^{n+1} \\ V_{sr}^{n+1} \\ V_{sj}^{n+1} \end{bmatrix} = \begin{bmatrix} W_a & -D_a & 0 & K_{aa} & 0 & 0 \\ D_a & W_a & -K_{aa} & 0 & 0 & 0 \\ 0 & K_{ac} & W_c & -D_c & 0 & K_{sc} \\ -K_{ac} & 0 & D_c & W_c & -K_{sc} & 0 \\ 0 & 0 & 0 & K_{ss} & W_s & -D_s \\ 0 & 0 & -K_{ss} & 0 & D_s & W_s \end{bmatrix} \begin{bmatrix} V_{ar}^n \\ V_{aj}^n \\ V_{cr}^n \\ V_{cj}^n \\ V_{sr}^n \\ V_{sj}^n \end{bmatrix} + \begin{bmatrix} -B \cdot V_{br}^n \\ -B \cdot V_{bj}^n \\ 0 \\ 0 \\ G \cdot V_{gr}^n \\ G \cdot V_{gj}^n \end{bmatrix}$$

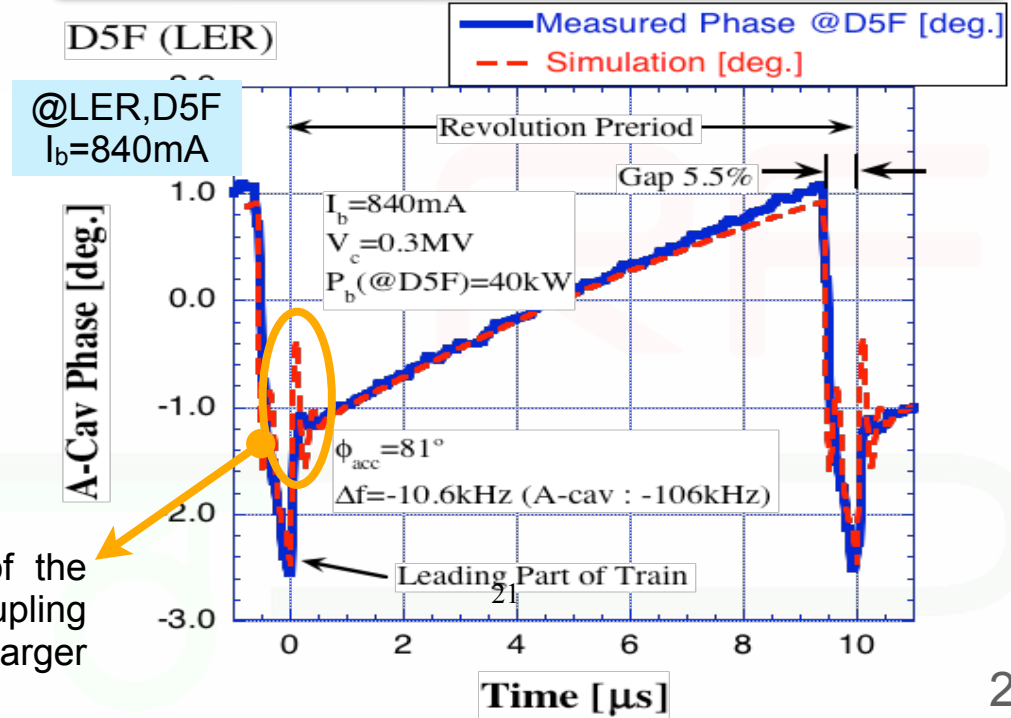
$$\begin{cases} \Delta\omega_\mu = \omega_\mu - \omega_{rf}, & \omega_{\mu/2} = \frac{\omega_\mu}{2Q_\mu}, \\ G = 2\sqrt{\beta_s} \Delta t \cdot \omega_{s/2}, & C = \sqrt{\beta_s}, \quad B = \Delta t \cdot \omega_{a/2}, \\ W_a = 1 - \Delta t \cdot \omega_{a/2}, & W_c = 1 - \Delta t \cdot \omega_{c/2}, \\ W_s = 1 - (\beta_s + 1) \cdot \Delta t \cdot \omega_{s/2}, & D_\mu = \Delta t \cdot \Delta\omega_\mu, \\ K_{\mu\nu} = \frac{k_\mu}{2} \cdot \Delta t \cdot \omega_{\nu/2} \cdot Q_\nu = \frac{k_\mu \cdot \Delta t \cdot \omega_\nu}{4}, \\ \mu, \nu : a, c, s, \end{cases}$$

Q-value of A-cavity ( $Q_a$ )	26000
Q-value of C-cavity ( $Q_c$ )	100
Q-value of S-cavity ( $Q_s$ )	180000
Coupling between A and C cavity ( $k_a$ )	5%
Coupling between S and C cavity ( $k_s$ )	1.6%

Simulation result agrees well with the measurement.

The behavior of the phase ringing at the head of the bunch train depends strongly on Q-value of the coupling cavity of ARES: Larger Q-value of C-cav. makes larger phase ringing at the train head.

A-Cavity Phase measured by new LLRF System in this SuperKEKB commissioning

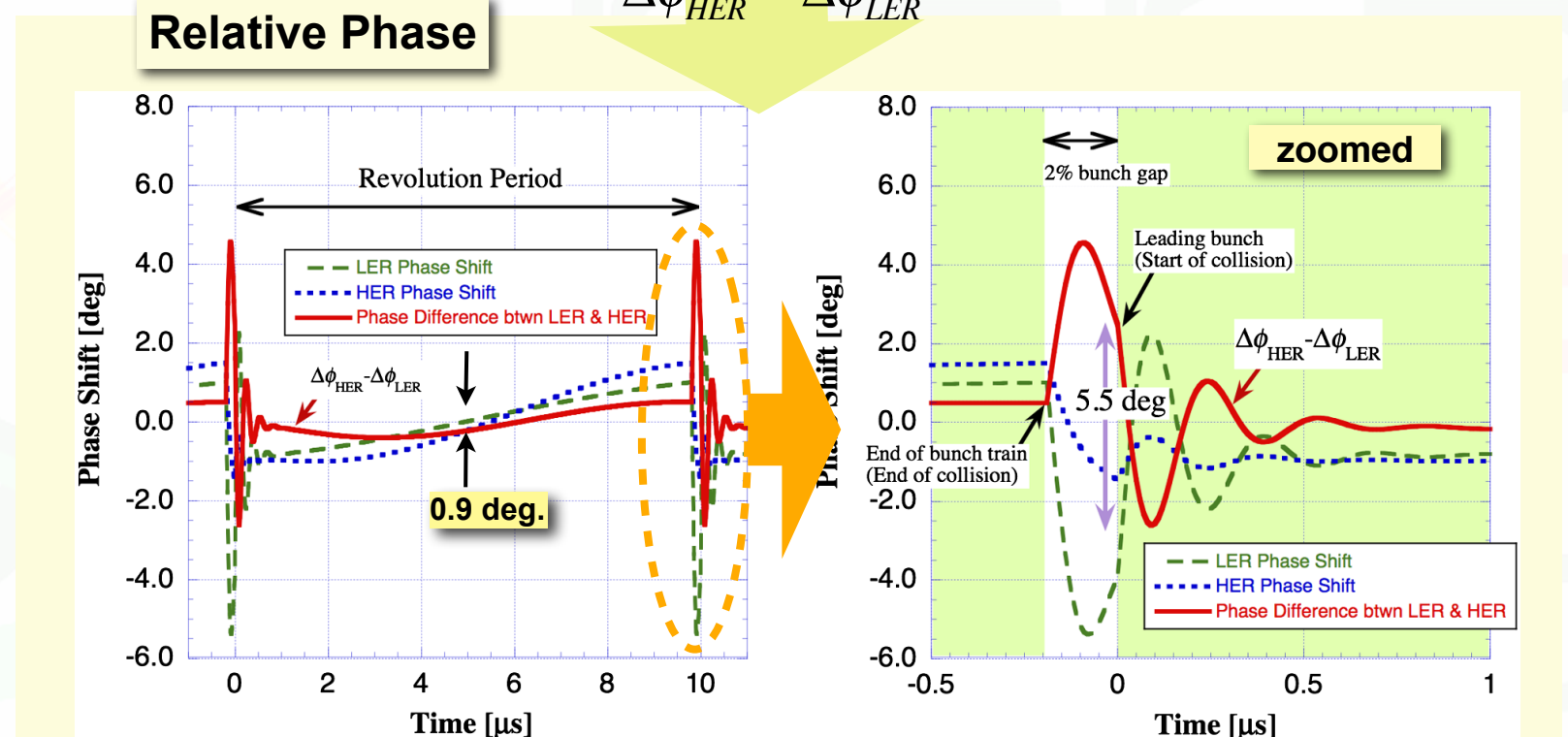
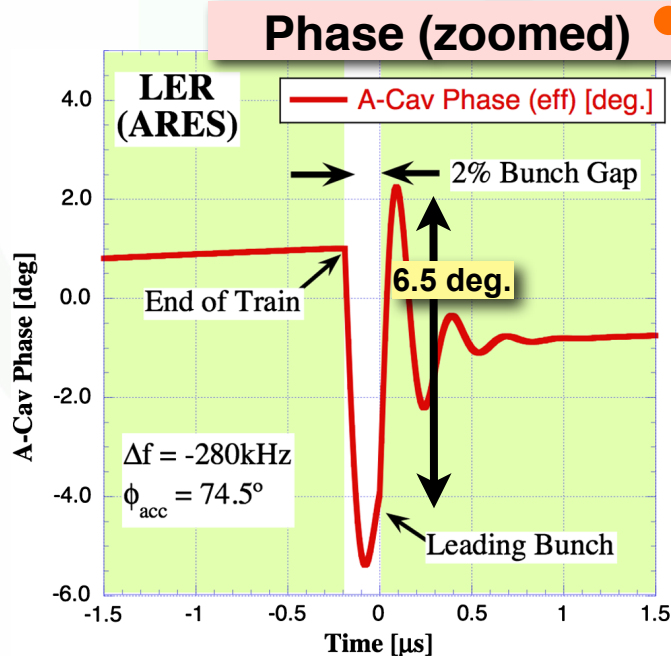
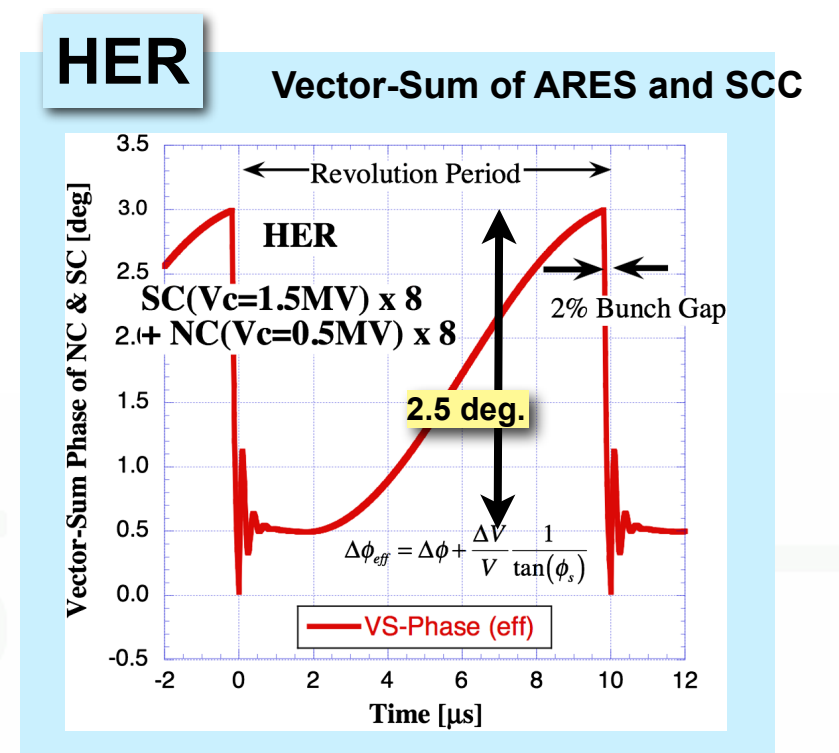
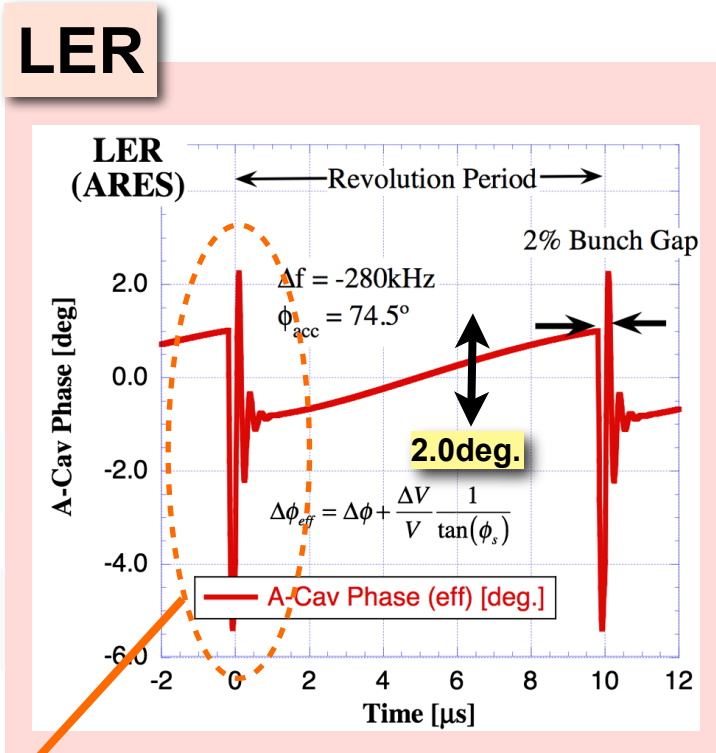


# Estimation of BGT for Design Current

LER:  $I_b=3.6$  A  
 HER:  $I_b=2.6$  A

Gap 2% (200ns)

Parameter	LER	HER
Beam energy [GeV]	4	7
Beam current [A]	3.6	2.6
Bunch gap length [%]	2	2
Beam power [MW]	8	8.3
Bunch length [mm] (rms)	6	5
RF frequency [MHz]	508.887	
Harmonic number	5120	
Revolution frequency [kHz]	99.4	
Cavity type	ARES	SCC/ARES
Number of cavities	22	8/8
Total RF voltage [MV]	10~11	15~16
Loaded Q of cavity [ $\times 10^4$ ]	2.4	7.0/2.0
Coupling factor ( $\beta$ )	4.3	-/5
RF voltage/cavity [MV]	0.48	1.5/0.5
Wall loss/cavity [kW]	140	-/150
Beam power/cavity [kW]	460	400/600
Cavity detuning [kHz]	-28	-18/-44
(A-Cav detuning of ARES)	(-280)	(-180)
Number of klystrons	18	8/8
Klystron power [kW]	~600	~450/~800



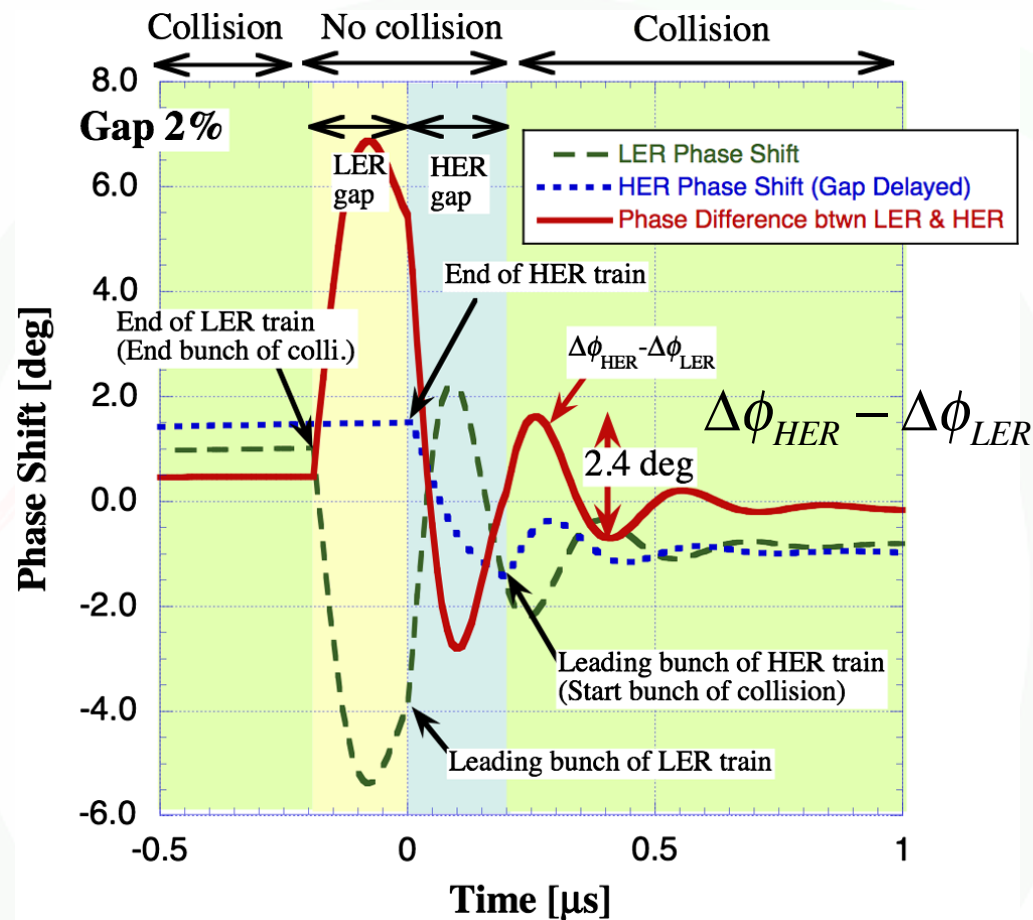
5.5 deg. -> Displacement@IP :  $0.44 \sigma_z$

# Measures to reduce phase difference (1)

Considering that the phase change due to the BGT effect will be critical for the high luminosity, measures are proposed to mitigate the phase difference between the colliding beams as a cure.

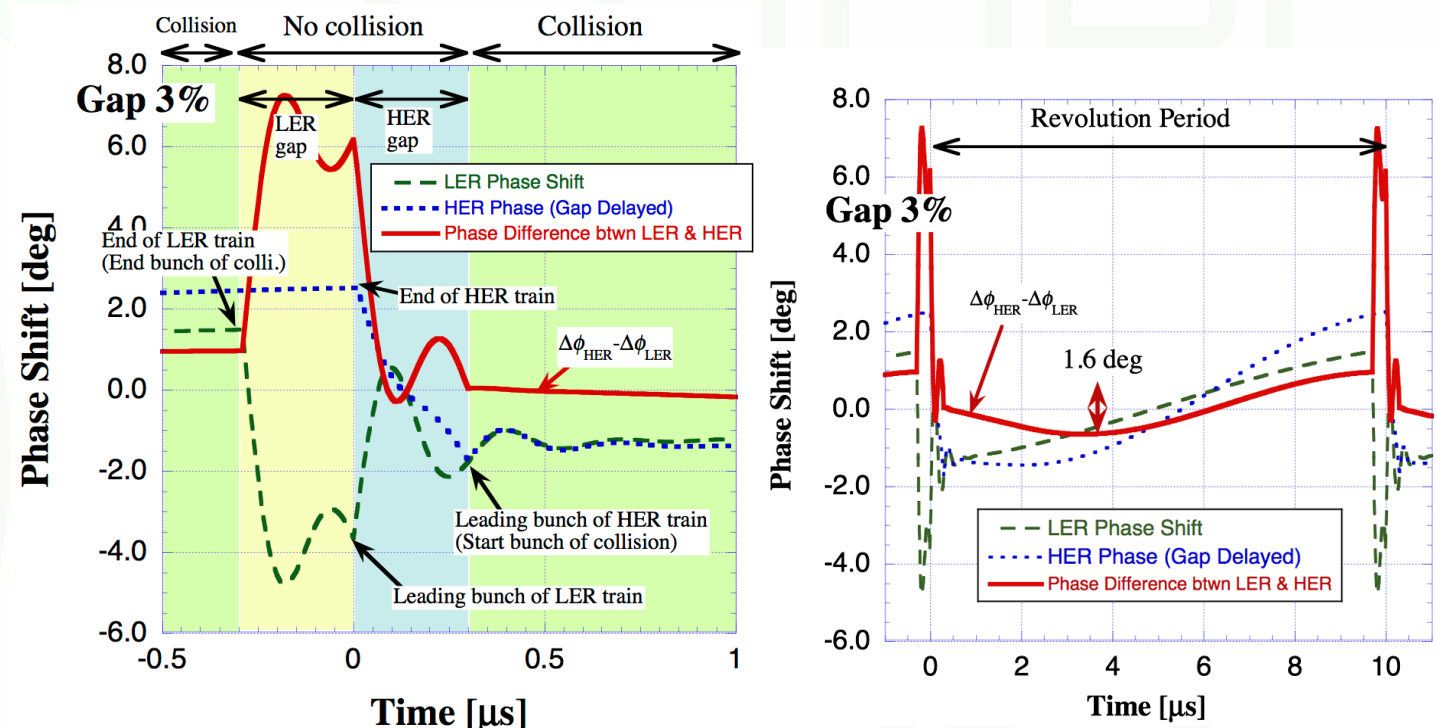
As a simple method, making a delay of the HER gap timing with respect to the LER gap is considered at the cost of a reduction of number of colliding bunches.

## Case of making 200-ns. gap delay in HER



In this case, the collision avoids the largest rapid phase change at the LER leading bunches. Then, the phase difference for the collision is reduced to 2.4 degrees from 5.5 for the collision. However, colliding bunches is reduced to 4% bunch gap equivalent.

## Case of 3% gap and 300-ns. HER gap delay



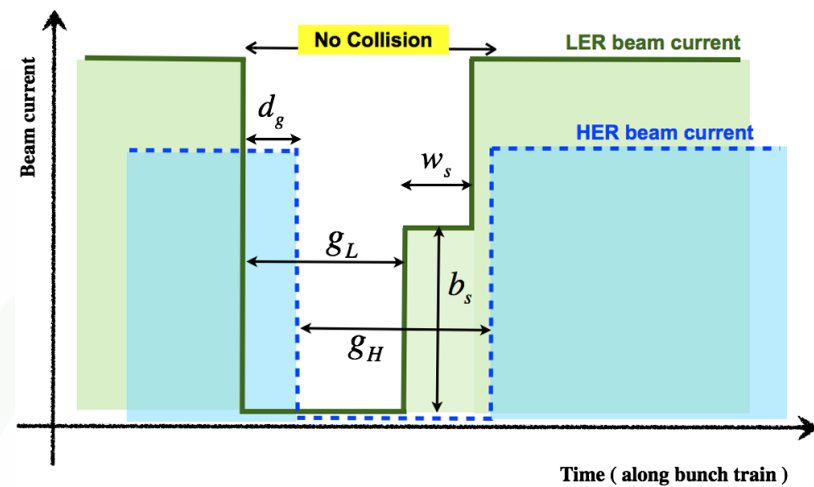
In this case, the phase difference between the two beams almost cancels at the leading part of the train. However, the phase difference along the entire bunch train in the revolution period is increased to 1.6 degrees from the no-delay case.

# Measures to reduce phase difference (2)

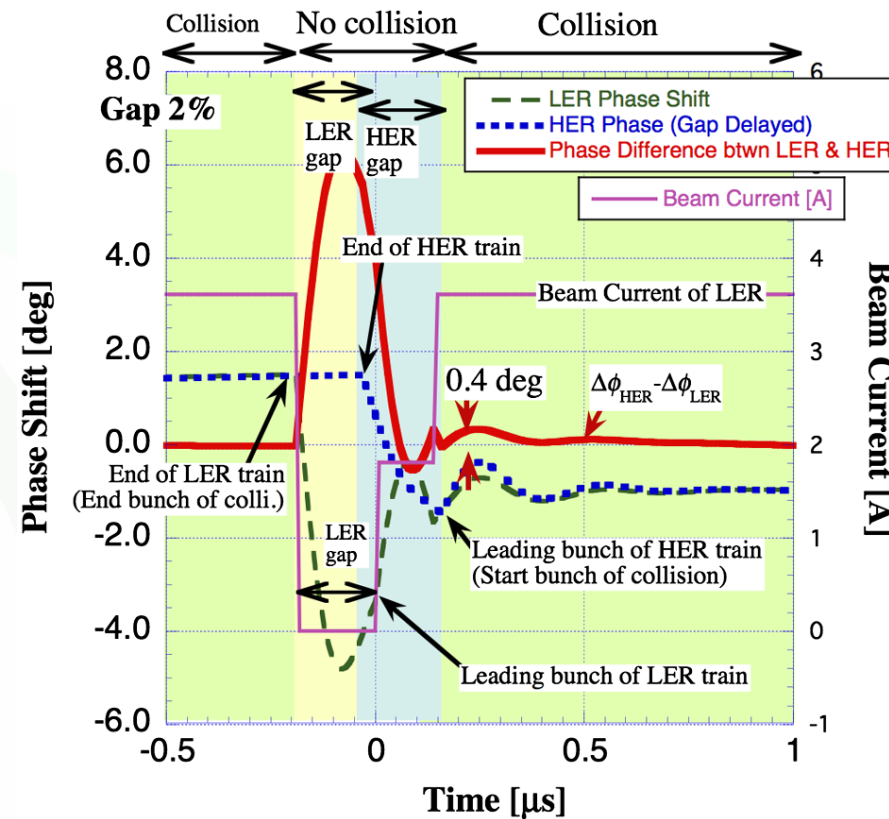
As a next method, changing the bunch fill pattern of LER is investigated for the mitigation.

**LER bunch train is filled up in two steps with HER gap delay.**

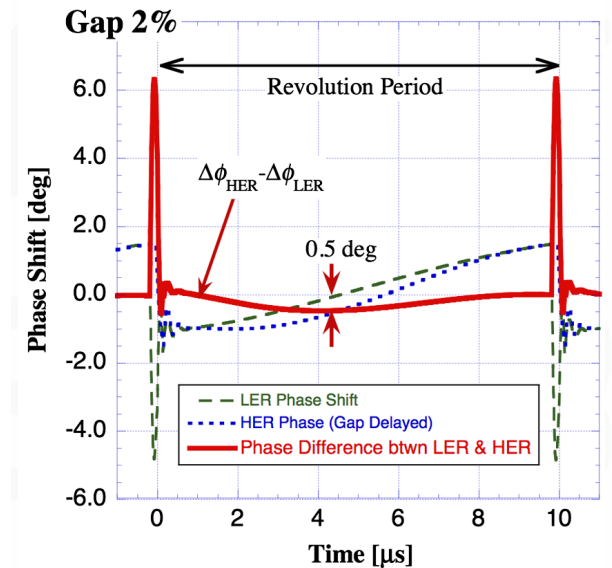
For the simplest case, the first step increase ( $b_s$ ) is set to half of the nominal bunch current.



Then, the HER gap delay and the time interval of the first step ( $w_s$ ) are parameters to be optimized.



$g_H = 160\text{ns}$   
 $w_s = 140\text{ns}$



Summary of effects of the proposed mitigation methods.

Method	Bunch gap	HER delay	Phase difference ( $ \Delta\phi_{\text{HER}} - \Delta\phi_{\text{LER}} $ ) [degrees]		Longitudinal displacement @IP ( $\sigma_z = 5\text{ mm}$ )	Rate of num. of colliding bunches
			Leading part	The rest of train		
HER gap delay	2%	no delay	5.5	0.9	$0.44 \sigma_z$	-
	2%	2% (200 ns)	2.4	0.9	$0.19 \sigma_z$	-2%
	3%	3% (300 ns)	< 0.2	1.6	$0.13 \sigma_z$	-4%
LER 2 steps + HER gap delay	2%	160 ns	0.4	0.5	$0.07 \sigma_z$	-1.6%

As the result, the phase difference between two rings is significantly reduced to 0.4 degrees at the leading part of the collision, while the entire phase difference along the train is kept sufficiently small.

It is an example of certain conditions.

In reality, the optimization depends on strongly operation conditions. The operation conditions will be optimized for the luminosity in future SuperKEKB.

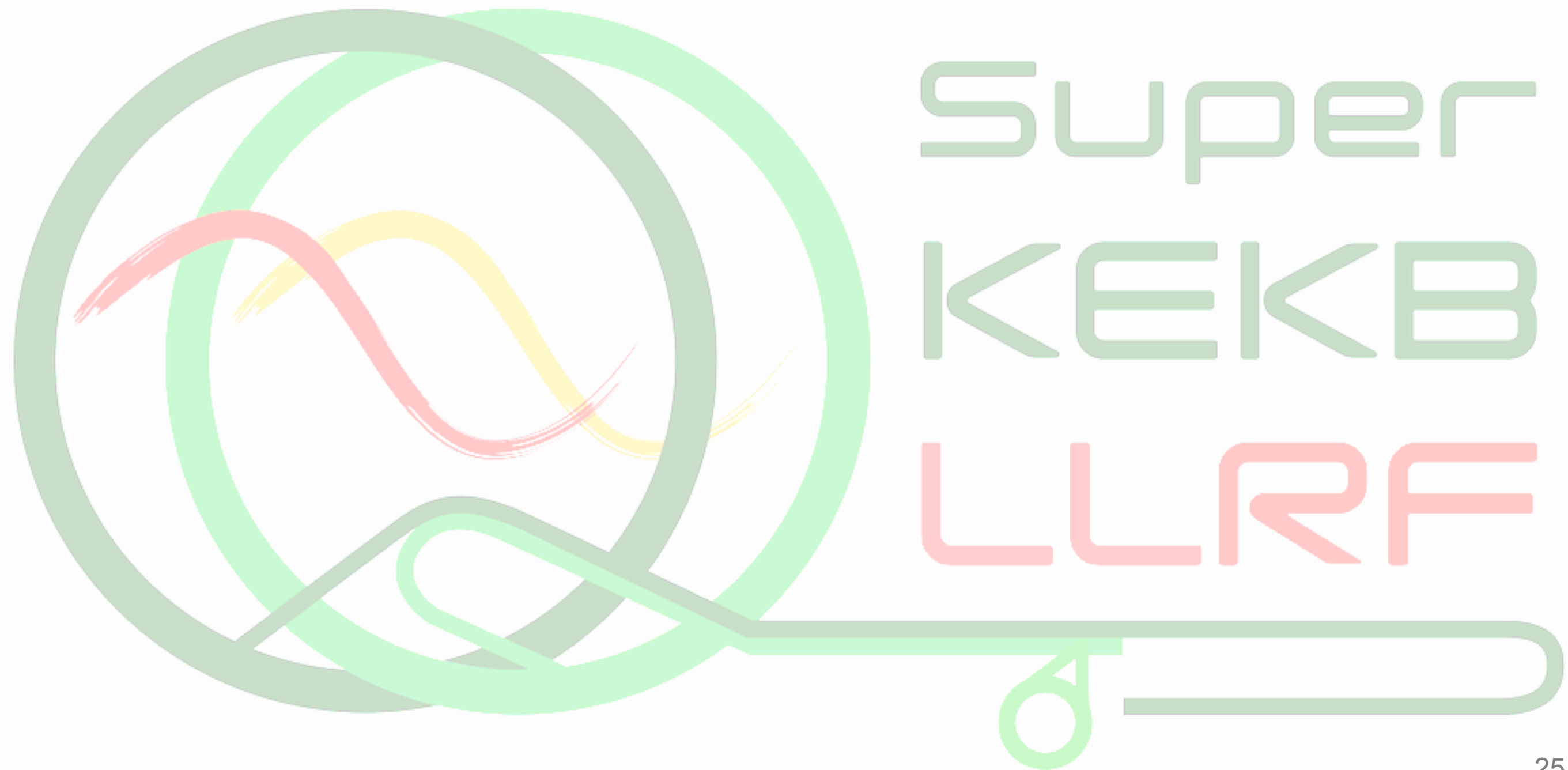
The best optimization for the fill pattern and gap delay will be investigated based on the best operation conditions.

The LER fill pattern change with a HER gap delay gives a more effective mitigation compared with only the gap delay cases.

# Summary

- RF system has been successfully operated without fatal problem, except several stations are powered off and put out of operation for variety reasons. Many old components and modules were repaired or replaced with spares
- Newly developed digital LLRF control systems are applied to 9 stations at OHO section, and successfully working.
- The  $\mu=-1$  mode damper is applied to HER, and the coupled bunch instability due to detuned cavities is suppressed successfully. The  $\mu=-2$  mode damper system is now under development for Phase-2.
- Phase modulation due to bunch gap transient effect will be too large at the leading part of the bunch train for design beam current.  
--> Simulation study proposes the measures to mitigate the phase difference: the relative phase change at the IP can be reduced by optimization of the gap delay and bunch fill pattern of LER.

**Tank you  
for your attention!**



# Backup Slides

SUPER  
KEKB  
RF

# RF Related Parameters (design value)

Parameter	unit	KEKB (achieved)				SuperKEKB (design)			
		HER		LER		HER		LER	
Ring		HER		LER		HER		LER	
Energy	GeV	8.0		3.5		7.0		4.0	
Beam Current	A	1.4		2		2.6		3.6	
Number of Bunches		1585		1585		2500		2500	
Bunch Length	mm	6-7		6-7		5		6	
Total Beam Power	MW	~5.0		~3.5		8.0		8.3	
Total RF Voltage	MV	15.0		8.0		15.8		9.4	
		ARES		SCC		ARES		SCC	
Number of Cavities		10	2	8	20	10	8	8	14
Klystron : Cavity		1:2	1:1	1:1	1:2	1:1	1:1	1:2	1:1
RF Voltage (Max.)	MV/cav.	0.5		1.5		0.5		1.5	
Beam Power (Max.)	kW/cav.	200	550	400	200	600	400	200	600

## Issues for RF systems

- Beam current will be twice of KEKB.
- Beam power/cavity will be 3 times higher than KEKB for ARES cavity.
- Bunch length will be shorter than KEKB. HOM Power will be increased.



Reinforce and reconfiguration of RF system is required.

# Instability due to RF cavities and cure

T. Kageyama, 2011.02

Ring	Longitudinal/Transverse	Cause	Frequency (MHz)	Growth time (ms)	Cure
LER	Longitudinal	ARES-HOM	1850	12	B-by-B FB
		ARES-0/ $\pi$	504	21	B-by-B FB
		-1 mode	508.79	4	-1 mode damper
LER	Transverse	ARES-HOM	633	7	B-by-B FB
HER	Longitudinal	ARES-HOM	1850	59	(no need)
		SCC-HOM	1018	58	(no need)
		-1 mode	508.79	4	-1 mode damper
HER	Transverse	ARES-HOM	633	39	(no need)
		SCC-HOM	688	14	B-by-B FB

Longitudinal bunch-by-bunch FB will be needed to suppress coupled bunch instabilities driven by RF cavities.

# RF Power for Ultimate Stage

T. Kageyama, 2011.02

SuperKEKB  $L = 8 \times 10^{35} \text{ cm}^{-2}\text{s}^{-1}$

HER SCC

$V_c$	1.5 MV
$P_{\text{beam}}$	400 kW

$e^- \rightarrow$   
 7 GeV x 2.6 A  
 $V_c = 15 \sim 16 \text{ MV}$   
 $P_{\text{beam}} = 8.0 \text{ MW}$   
 by  
 8xARES + 8xSCC

$\leftarrow e^+$   
 4 GeV x 3.6 A  
 $V_c = 9.4 \text{ MV}$   
 $P_{\text{beam}} = 8.3 \text{ MW}$   
 by  
 22xARES

HER ARES

$V_c$	0.5 MV
$P_{\text{wall}}$	150 kW
$P_{\text{beam}}$	600 kW
Input $\beta$	5.0
$P_{\text{PMD}}$	21 kW

LER ARES	1 : 1	1 : 2
$V_c$	0.48 MV	0.34 MV
$P_{\text{wall}}$	140 kW	70 kW
$P_{\text{beam}}$	460 kW	230 kW
Input $\beta$	4.3	4.3
$P_{\text{PMD}}$	14 kW	7 kW

-  Klystron
-  SCC
-  ARES

D11  
NIKKO  
D10

D4  
OHO  
D5

D8  
FUJI  
D7

# 22 ARES Cavities operated for LER ( $I_b=3.6A$ )

T. Kageyama, 2011.02

RF frequency	508.869 MHz	
Flywheel Energy Ratio $U_S / U_A$	9	unchanged
Cavity Voltage $V_c$	0.48 MV	$P(\text{wall}) = 140 \text{ kW}$
Detuning Frequency $\Delta f_{\pi/2} / \Delta f_{AC}$	-28 kHz / -280 kHz	$P(\text{beam}) = 460 \text{ kW}$
Input Coupling Factor $\beta$	5.0	$\beta$ (optimum) = 4.3
CBI (-1 mode) due to the Acc. mode	$\tau = 4 \text{ ms}$	RF feedback
CBI due to the 0 and $\pi$ modes	$\tau = 21 \text{ ms}$	bunch-by-bunch FB

# HOM Power Estimation for LER

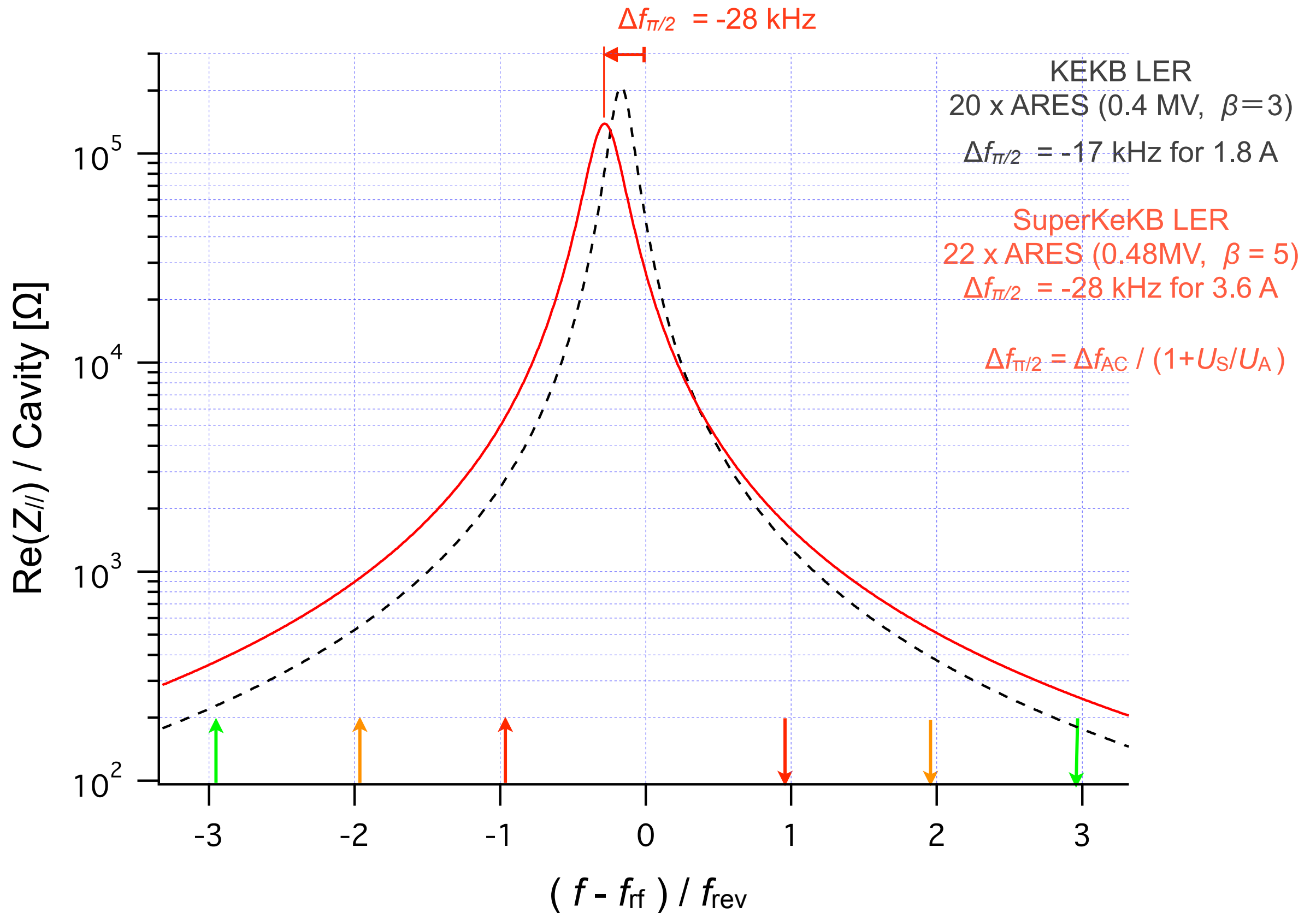
T. Kageyama, 2011.02

	KEKB LER Sep. 21, 2004	SuperKeKB LER	Power Handling Capability verified at 1.25 GHz	Factor of Safety
$I_{beam}$ [A]	1.6	3.6	-	-
$N_{bunch}$	1293	2503	-	-
$\sigma_z$ [mm]	7	6	-	-
$k$ [V/pC]	0.40 (0.39 <sup>†</sup> )	0.44	-	-
$P_{HOM}$ /ARES [kW]	5.4 <sup>†</sup>	17	-	-
$P_{HOM}$ /HWG [kW]	1.05 <sup>†</sup>	3.3	5.0	5.0/3.3 = 1.5
$P_{HOM}$ /Groove [kW]	0.3 <sup>†</sup>	0.93	1.2	1.2/0.93 = 1.3

<sup>†</sup>based on calorimetric measurement

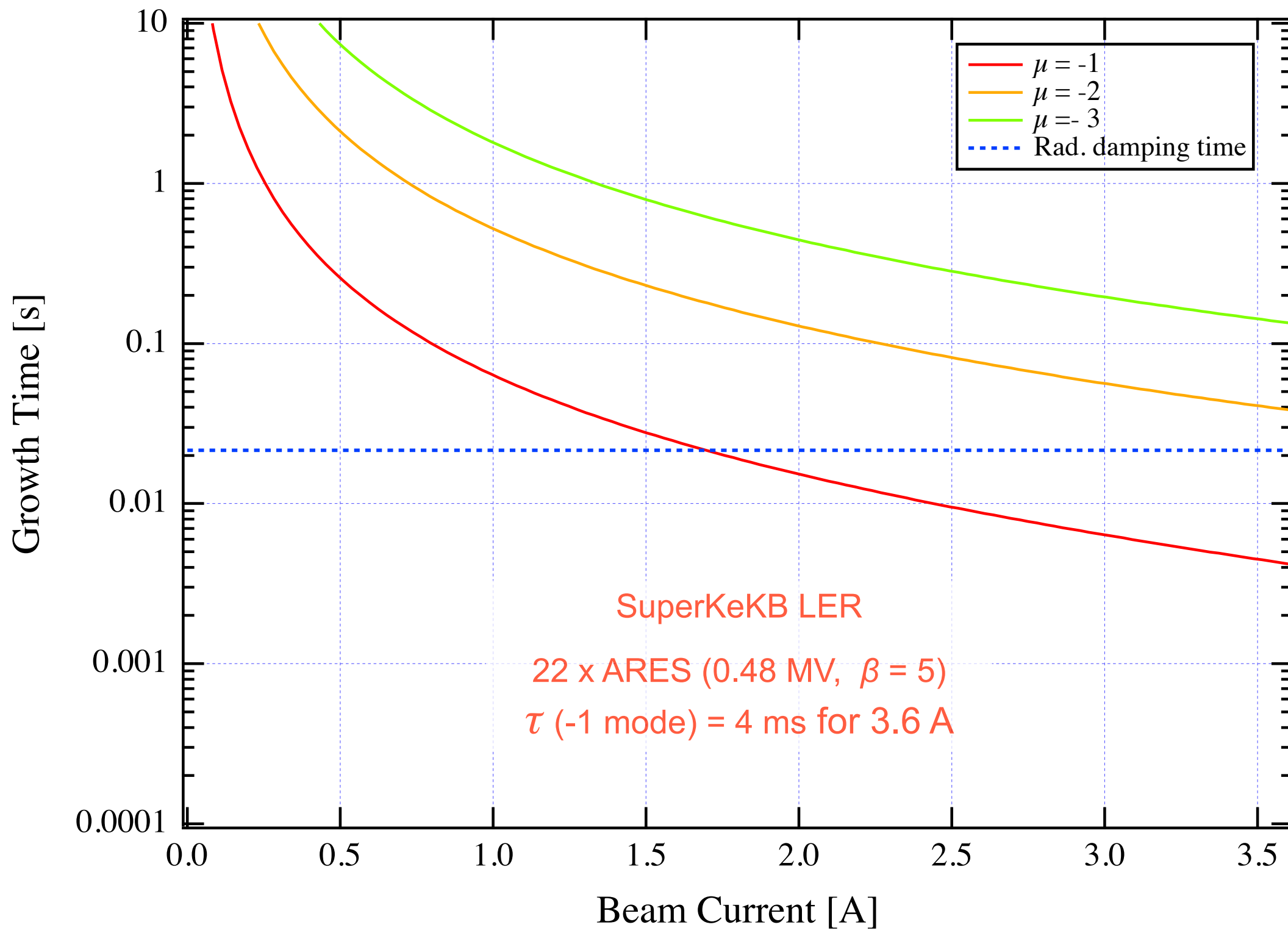
# Coupled Bunch Instability (CBI) driven by the Accelerating Mode ( $\pi/2$ )

T. Kageyama, 2011.02



# CBI due to the Accelerating Mode ( $\pi/2$ )

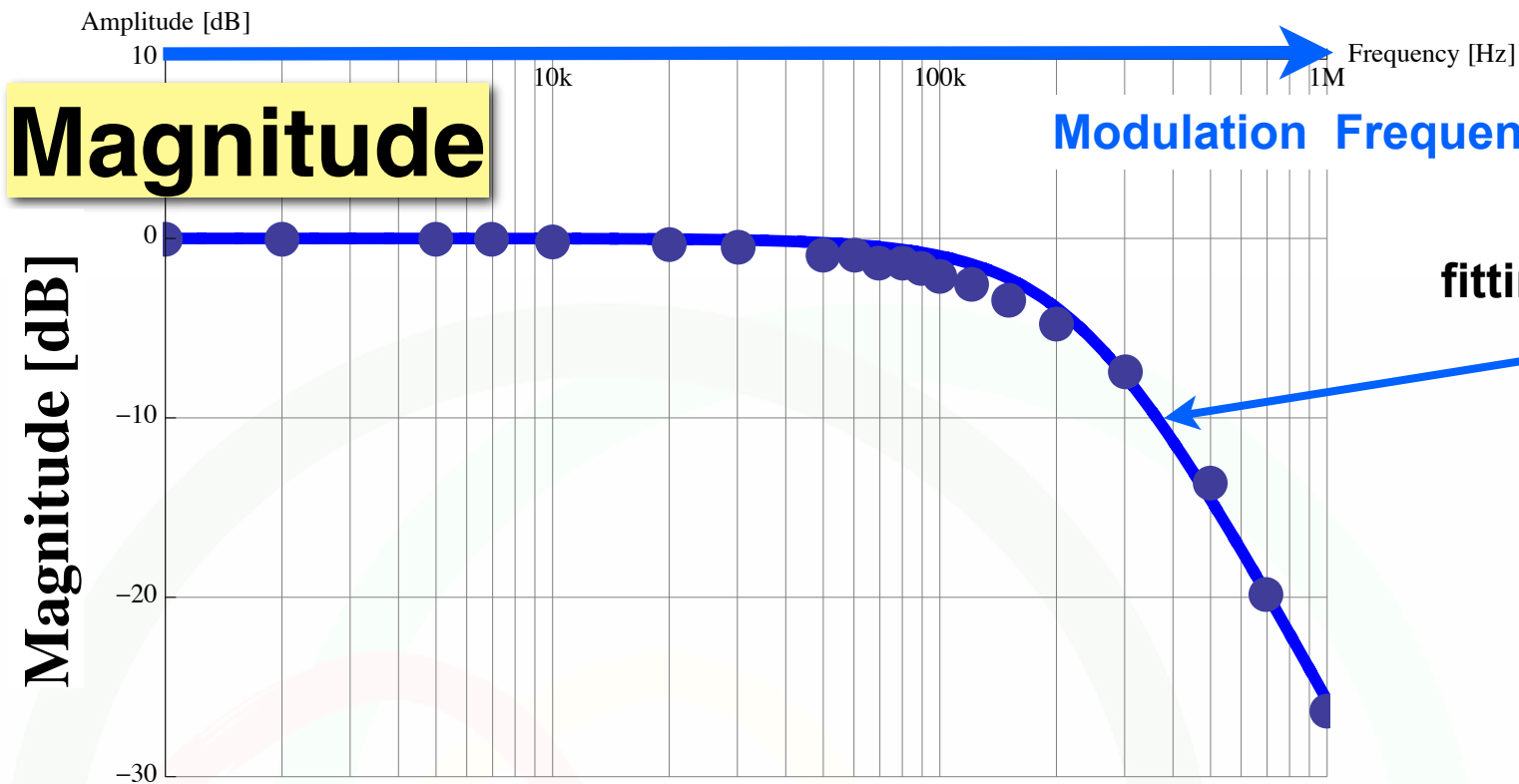
T. Kageyama, 2011.02



# Response Property - Klystron Bandwidth

(open loop)

## Measured Result



fitting curve with

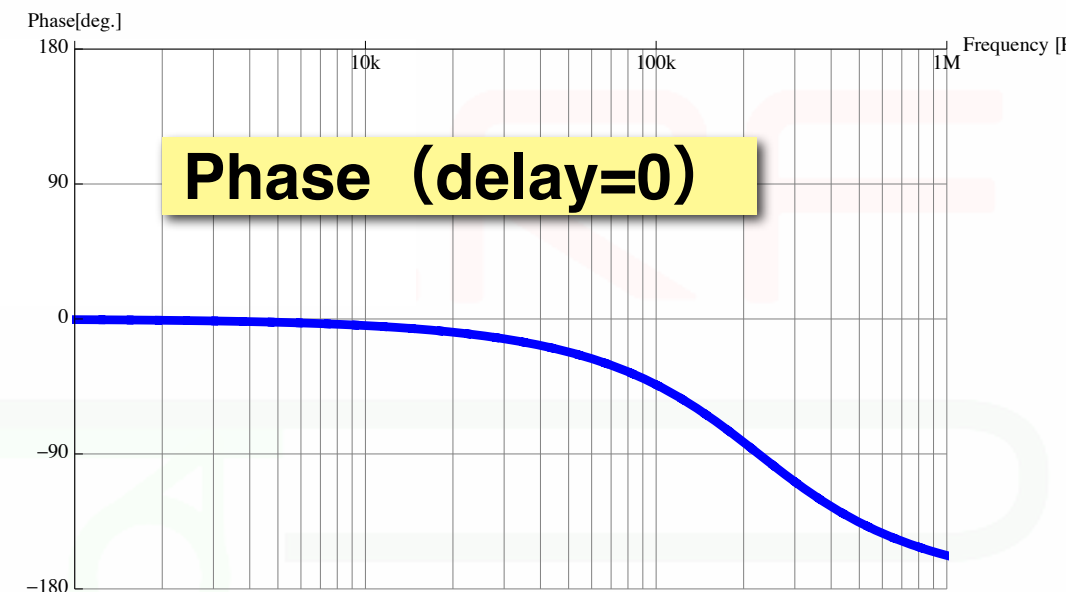
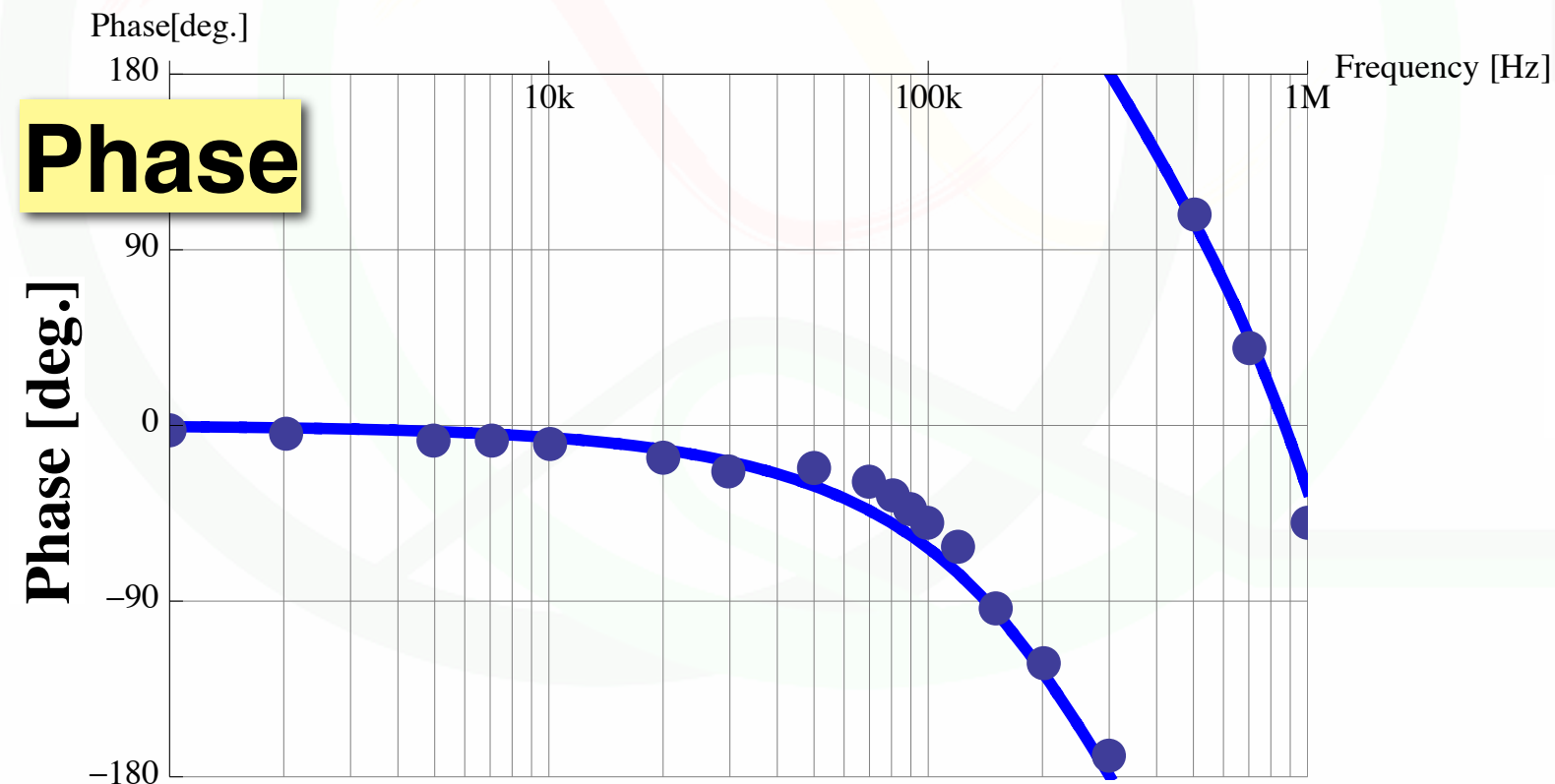
$$H_{kly}[s] = \frac{1}{1 + s/\omega_{kly} + s^2/\alpha} \cdot e^{-s \cdot T_d}$$

$T_d$  : Delay

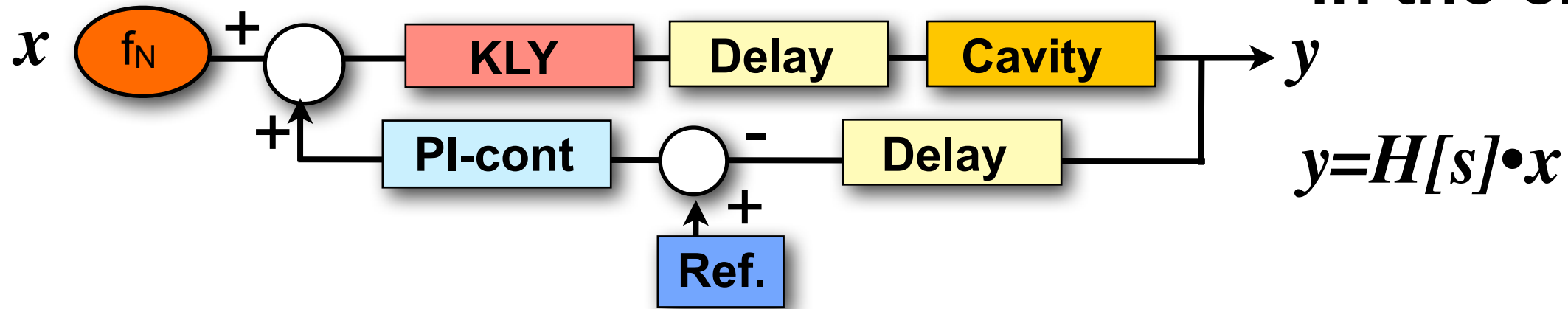
$\omega_{kly} = 130 \text{ kHz}$

$T_d = 650 \text{ ns}$

$\alpha = 2.1 \times 10^{12}$



# Disturbance Rejection Characteristics in the closed loop



## Magnitude ( $h_{11}$ )

## Calculation & Measurement

